View metadata, citation and similar papers at core.ac.uk

brought to you by CORE

provided by Scholarship at UWindsor

University of Windsor
Scholarship at UWindsor

Electronic Theses and Dissertations

2009

Quantum Phase Transition in Triple Quantum Dot System and Its Consequences on Transport

Behnam Javanparast
University of Windsor

Follow this and additional works at: http://scholar.uwindsor.ca/etd

Recommended Citation

Javanparast, Behnam, "Quantum Phase Transition in Triple Quantum Dot System and Its Consequences on Transport" (2009). *Electronic Theses and Dissertations.* Paper 374.

This online database contains the full-text of PhD dissertations and Masters' theses of University of Windsor students from 1954 forward. These documents are made available for personal study and research purposes only, in accordance with the Canadian Copyright Act and the Creative Commons license—CC BY-NC-ND (Attribution, Non-Commercial, No Derivative Works). Under this license, works must always be attributed to the copyright holder (original author), cannot be used for any commercial purposes, and may not be altered. Any other use would require the permission of the copyright holder. Students may inquire about withdrawing their dissertation and/or thesis from this database. For additional inquiries, please contact the repository administrator via email (scholarship@uwindsor.ca) or by telephone at 519-253-3000ext. 3208.

Quantum Phase Transition in Triple Quantum Dot system and its Consequences on Transport

by

Behnam Javanparast

A Thesis
Submitted to the Faculty of Graduate Studies
through the Department of Physics in Partial Fulfillment
of the Requirements for the Degree of Master of Science at the
University of Windsor

Windsor, Ontario, Canada
2009

© 2009 Behnam Javanparast

All Rights Reserved. No part of this document may be reproduced, stored or otherwise retained in a retrieval system or transmitted in any form, on any medium by any means without prior written permission of the author.

Author's Declaration of Originality

I hereby certify that I am the sole author of this thesis and that no part of this thesis has been published or submitted for publication.

I certify that, to the best of my knowledge, my thesis does not infringe upon anyone's copyright nor violate any proprietary rights and that any ideas, techniques, quotations, or any other material from the work of other people included in my thesis, published or otherwise, are fully acknowledged in accordance with the standard referencing practices. Furthermore, to the extent that I have included copyright material that surpasses the bounds of fair dealing within the meaning of the Canada Copyright Act, I certify that I have obtained a written permission from the copyright owner(s) to include such material(s) in my thesis and have included copies of such copyright clearances to my appendix.

I declare that this is a true copy of my thesis, including any final revisions, as approved by my committee and the Graduate Studies office, and that this thesis has not been submitted for a higher degree to any other University or Institution.

Abstract

In this thesis, possibility of quantum phase transition in systems composed of quantum dots will be studied. We also investigate the consequence of this phase transition on transport. We particularly consider a triple quantum dot system (three quantum dots sitting on the corners of an equilateral triangle) coupled to three leads symmetrically. To probe quantum phase transition we utilize slave-boson mean-field theory and to investigate transport properties we use scattering formalism. We detect a competition between Kondo and non-Kondo regime in this system. This competition affects transport in a way that conductance and noise will become zero when the non-Kondo regime dominates, in other words when the system crosses the phase boundaries. The results of this research can motivate experiments on the same systems to probe quantum phase transition and provides theoretical background for the experiment. It can also motivate future theoretical work using different methods from mean-field theory.

Acknowledgement

I 'd like take this opportunity to express my thanks for the assistance I received from various people. Firstly, I'd like to thank my friend Paul Moffatt for helping me with LaTeX and some numerical aspects of my project. I'd like to thank my friend Arathi Padmanabhan for helping me edit my writing. I'd also like to thank Dr. J. David Keselica for discussions which helped me during my calculations.

Most importantly I 'd like to express my thanks to my supervisor Dr. Eugene H. Kim for giving me the opportunity of working under his supervision. His lectures gave me a strong insight into the fundamentals of Physics and enhanced my motivation to find my desired field. It was a great pleasure for me to work with him in a research capacity.

Contents

Author's Declaration of Originality iii

Abstract iv

Acknowledgement v

List of Figures ix

1 Introduction 1

1.1 Quantum Dot: A Form of Artificial Atom 2

1.1.1 Models to Describe Quantum Dots 5

1.2 Impurity Problem, Kondo effect and Quantum Dots 7

1.2.1 Brief History 7

1.2.2 A Physical Description of the Kondo effect 9

1.2.3 Kondo effect in Quantum Dots 10

1.3 Phase Transitions 12

1.3.1 General Concepts 12

1.3.2 Universal Properties 14

1.3.3 Quantum Phase Transitions 16

1.4 In this Thesis 19

2 Effective Low Energy Hamiltonian and Analysis **21**

2.1 Low Energy Hamiltonian 21

2.1.1 From Anderson to Kondo 23

2.1.2 Slave-boson Analysis 26

2.2 Mean-Field Theory 32

2.2.1 Applying Mean-Fields 33

2.2.2 Calculating the Mean-Field Variables 35

2.3 Mean-Field Equations: Self-Consistent Solutions 41

3 Calculation of Transport **46**

3.1 Scattering Formalism and Triple-Dot Scattering Matrix 46

3.2 Conductance and Current-Current Correlation Function 52

3.2.1 Conductance 52

3.2.2 Current-Current Correlation Function 55

4 Conclusion **70**

A Hubbard-Stratonovich Transformation **72**

B Symmetries and Their Consequences **75**

B.1 Case of $\eta =< f^{\dagger}_{l+1\sigma} f_{l\sigma} >$: 75

B.2 Case of $\chi =< \psi^{\dagger}_{l\sigma} f_{l\sigma} >$: 76

C Relation between Spectral Density and Thermal Occupation **78**

D Integrals containing Fermi-Dirac Distribution Function **81**

E Numerical Calculations: Methods and Results **83**

References **88**

VITA AUCTORIS **91**

List of Figures

1.1 Schematic figure of a quantum dot. (a) is the view from top and (b) is a side view 3

1.2 Figure of our system, the bent lines represent leads, and black circles represent dots. t and t' are constants for electrons hopping from"dot to dot" and from "lead to dot or dot to lead". 4

1.3 Red curve represents "Kondo effect", Blue curve "resistance saturation, and Green one "superconductivity". 7

1.4 Anderson model of magnetic impurity [1]. (a) shows that energy level of impurity is below the Fermi level of the host metal ε_0 It costs U to add another electron to the impurity which is not favourable. (b) shows that the impurity electron tunnels out. (c) electron from host metal tunnels in. In this case spin of electron has flipped and a singlet has formed between electron in the impurity and the electron in "resonant level. 9

1.5 Density of states of impurity atom, the (extra) peak at the Fermi energy is due to the formation of the Kondo resonance. 11

2.1 Figure of our system, the bent lines represent leads, and black circles represent dots. t and t' are constants for electrons hopping from"dot to dot" and from "lead to dot or dot to lead". 22

2.2 examples of high energy configurations which has been integrated out. In each corner (which practically is a quantum dot) the number of electrons has been shown. 25

2.3 (a) shows processes which fourth term of low energy Hamiltonian (2.8 represents, Kondo effect, one electron from a quantum dot tunnels out and another electron tunnels in and both happens at the same corner. Spin flip can also happen. (b) represents the fifth term. It is basically the same process as (a) but tunnelling in and tunnelling out happens at different corners. 27

2.4 Blue Graph Represent $\Gamma = \pi\rho_0 V_0^2$ where V_0 depends on mean-field variable χ. The dashed red line represents mean-field variable η. By tuning J a quantum phase transition will happen.($t = 4J$) By tuning the coupling constants, a competition will happen between two states. One is the state of singlet between the electron on the dot and the virtual bound state in the lead. The other is formation of singlet between two neighbour dots. At the poit of phase transition which we can see in the graph, the second phase (neighbour dot singlet) gets dominant knowing that before that particular point (particular value of J) the first phase ("Kondo singlet") was dominant.By tuning the coupling constants, a competition will happen between two states. One is the state of singlet between the electron on the dot and the virtual bound state in the lead. The other is formation of singlet between two neighbour dots. At the poit of phase transition which we can see in the graph, the second phase (neighbour dot singlet) gets dominant knowing that before that particular point (particular value of J) the first phase ("Kondo singlet") was dominant. 42

2.5 Blue Graph Represent $\Gamma = \pi\rho_0 V_0^2$ where V_0 depends on mean-field variable χ. The dashed red line represents mean-field variable η. By tuning J a quantum phase transition will happen.$t = 10J$ 43
2.6 Blue Graph Represent $\Gamma = \pi\rho_0 V_0^2$ where V_0 depends on mean-field variable χ. The dashed red line represents mean-field variable η. By tuning J a quantum phase transition will happen.$t = 17J$ 44

3.1 Schematic figure of 1 dimensional scattering 47
3.2 (a) representation of one lead. (b) representation of our system with the (a) substitution. Big black circle represent the triple-dot system which is also the scatterer. The spatial extention of the leads of our system in this picture is from $-\infty$ to $+\infty$, but the extention of the leads are actually form $-\infty$ to the dot. The extended part represents the section which reflected particles enter. The structure of the triple dot does not appear in this picture, but in calculations this structure will be taken into account. 51
3.3 Conductance of Drains,$t = 4J$ 56
3.4 Conductance of Drains,$t = 10J$ 57
3.5 Conductance of Drains,$t = 17J$ 58
3.6 Non-zero current-current correlations in Case 1, $t = 4J$ 64
3.7 Non-zero current-current correlations in Case 2, $t = 4J$ 65
3.8 Non-zero current-current correlations in Case 1, $t = 10J$ 66
3.9 Non-zero current-current correlations in Case 2, $t = 10J$ 67
3.10 Non-zero current-current correlations in Case 1, $t = 17J$ 68
3.11 Non-zero current-current correlations in Case 2, $t = 17J$ 69

Chapter 1

Introduction

Investigation in Mesoscopic systems [1] is one of the most active areas in contemporary physics. Nanostructures like quantum dots[3], carbon nanotubes[4], etc have been built and have been used to make devices which have important influences on many areas in physics such as foundation of quantum mechanics [5] [6] [7] quantum information [8] [9] [10] and condensed matter physics [11]. Rapid progress in microfabrication technology makes it possible to manufacture devices composed of different combinations of these nanostructures. Therefore theoretical investigations in these kinds of systems and getting laboratory testable results have considerable importance.

Recently investigations in systems composed of coupled quantum dots in which dots are coupled to the metallic lead, have been attracting attention of both theoretical and experimental physicists. The couplings between the dots as well as the couplings between a dot and a lead can be controlled; as a result, a variety of states/phase

[1] The terminology "mesoscopic systems" is very often used for the same systems as nanoscale structures or nanoscale devices. Here nano means a size on the order of several nanometers, namely, $10^{-9}m$. In other words, the systems corresponds to a scale of less than one micrometer, $10^{-6}m$.[2]

can arise. Furthermore, by tuning the couplings, one can drive a competition between these states/phases, giving rise to a (quantum) phase transition.

Quantum phase transitions have been investigated and observed in cases of two magnetic impurities in metal or two-coupled dot systems. In this thesis we will consider a system composed of three quantum dots sitting on the corners of an equilateral triangle. As mentioned, they are coupled to each other and are coupled to three leads symmetrically. We probe conditions of quantum phase transitions occurrence and its consequences on transport. In the rest of this introduction, we discuss the system(s) and the physics motivating the work done in this thesis.

1.1 Quantum Dot: A Form of Artificial Atom

Artificial atoms are "Particles of metals or 'pools' of electrons in a semiconductor that are a few hundred angstroms in size" [3] . These mesoscopic structures have discrete number of electrons and have discrete energy levels like any natural atoms. Metallic gates or material boundaries(like pieces of insulators) play the role of the nuclear charge in artificial atoms. Electrons will be confined in a small region using insulators in the case of metallic particles or using electric field in the case of semiconductor pools[2]. The fabrication of these structures is accomplished by the techniques of electron or X-ray lithography [3].

There are many forms of artificial atoms. All-metal, controlled-barrier and quantum dots. Quantum dots come in different geometries [12] like rods, pancakes,... . We are generally interested in quantum dots regardless of their shapes.

Quantum dots are ultimate in confinement of electrons. They contain mobile electrons in a "box" [12]. The confinement, as mentioned earlier, is provided by insulation or electric field. (figure 1.1)

[2]There are also categories of quantum dots which use different mechanism of confinement of electrons [4]

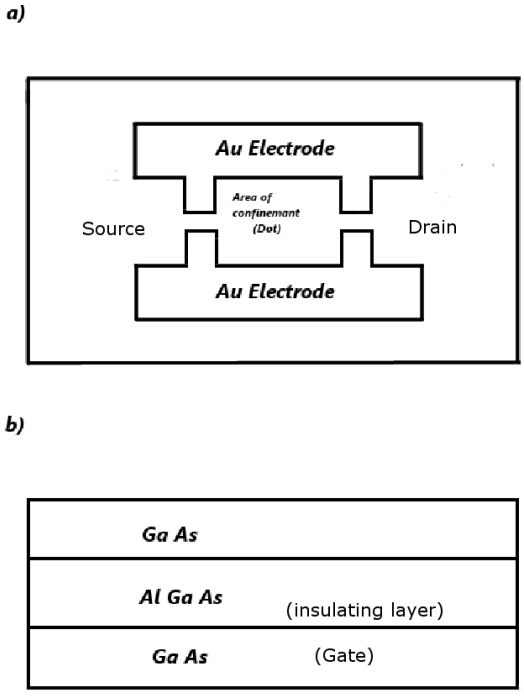

Figure 1.1: Schematic figure of a quantum dot. (a) is the view from top and (b) is a side view

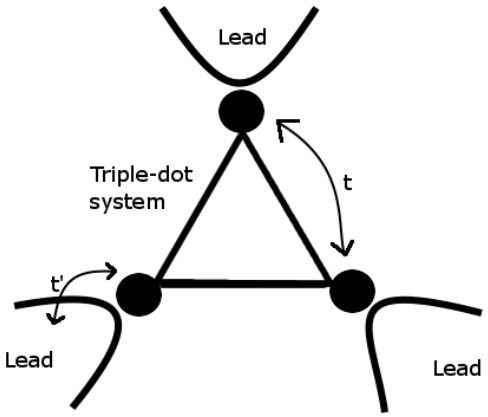

Figure 1.2: Figure of our system, the bent lines represent leads, and black circles represent dots. t and t' are constants for electrons hopping from"dot to dot" and from "lead to dot or dot to lead".

In the case of a strong enough confinement and small enough size of the box, quantum effects such as tunnelling can be observed macroscopically and consequently the possibility of interesting phenomena like transport through quantum dots will be brought up.[13] [14] [15] [16]

One of the most interesting applications of quantum dots involves devices in which several quantum dots are coupled. Because the coupling of the quantum dots can be controlled and be adjusted, interesting physics can be observed in these multiple quantum dot systems. In our research, we have considered a system composed of three coupled quantum dots sitting on the corners of an equilateral triangle. (figure 1.2)

1.1.1 Models to Describe Quantum Dots

As we mentioned earlier, artificial atoms behave like natural atoms in a sense that they have quantized charge and quantized energy levels. First model which gives a fairly comprehensive description of the situation was Coulomb blockade model. This model describes sharp peaks in conductance diagram of a quantum dot for different gate voltages using the fact that in order to add charge Q to a quantum dot with no charge and no bias voltage between its source and drain, we need an energy $\frac{Q^2}{2C}$ where C is the total capacitance between the dot and the rest of the system. If the electron can tunnel back and forth this means you have current and as a result you can measure the conductance. Since the least value of Q is e, the flow of current at least requires a "Coulomb energy" $\frac{e^2}{2C}$. This energy barrier is called Coulomb blockade. The electron in the lead has to have an energy difference by $\frac{e^2}{2C}$ above the Fermi level of the dot to be able to tunnel to the dot.[3] So quantization of charge causes energy gap in the spectrum of states for tunnelling.

Total electrostatic energy of dot after adding charge Q will be $E = QV_g + \frac{Q^2}{2C}$. Because we are dealing with electrons $Q < 0$ and we use a positive gate voltage (to attract electrons), the expression of E has a minimum. By changing the gate voltage the minimum of E changes as well and for a certain point (minimum), the system will have no preference for either adding or subtracting an electron to the dot. At this point the peaks in conductance of a quantum dot will happen.

Since quantum dots are composed of metals or semiconductors and they are coupled to metallic leads as sources of electrons, condensed matter models which include more details about the system under study, can be utilized to obtain more quantitative results such as transmission probability, tunnelling rates and coupling constants. One of the most important condensed physics models which has been vastly used to

[3] same argument applyies for the holes but below the Fermi surface of the dot and this represents tunnelling out of the dot.

explain quantum dots is Anderson model [17] [18]. As an example, we mention the Hamiltonian of a quantum dot coupled to two metallic lead :

$$H = \sum_{d\sigma} \varepsilon_d c^\dagger_{d\sigma} c_{d\sigma} + \sum_{lp\sigma} \varepsilon_p c^\dagger_{lp\sigma} c_{lp\sigma} + t \sum_{dl\sigma} \psi^\dagger_{l\sigma}(0) c_{d\sigma} + c^\dagger_{d\sigma} \psi_{l\sigma}(0) \tag{1.1}$$

where $\psi_{l\sigma}$ is :

$$\psi_{l\sigma}(0) = \frac{1}{\sqrt{V}} \sum_p c_{lp\sigma} \tag{1.2}$$

In equation 1.1 first term describes quantum dot, second term describes the leads and third term shows the contact between leads and quantum dot.$\psi_{l\sigma}$ is a second quantized operator which describes electrons in the leads and $c_{d\sigma}, c_{lp\sigma}$ are annihilation operators in the dot and leads (in order) and t is the coupling constant.

This model is usually applied to the case of quantum dots only in certain regime of its parameters, known as finite-U Anderson model. U represents the Coulomb interaction between electrons in the dots. This allows to treat some of the terms in the Hamiltonian as a perturbation. Anderson-like Hamiltonians are the start point for many theoretical calculations related to the systems composed of one or more quantum dots. Many theoretical techniques such as mean field theory, renormalization group [19] have been developed to tackle problems related to these systems and many interesting physical phenomena has been observed and predicted [20] [21] [22]. Therefore we also expect to detect some of these phenomena in quantum dot systems [23] [16] and we can apply the developed techniques as well[24].

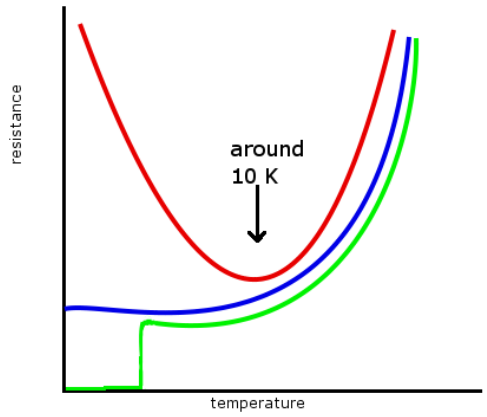

Figure 1.3: Red curve represents "Kondo effect", Blue curve "resistance saturation, and Green one "superconductivity".

1.2 Impurity Problem, Kondo effect and Quantum Dots

1.2.1 Brief History

In most (three dimensional) metals resistivity monotonically decreases with decrease of temperature [19] because of the decrease of phonon scattering. In this process some of them become superconductors and some of them reaches a saturated value of resistance [1]. During 1930s a resistance minimum was observed in some metals. This minimum was caused by impurities associated with 3d transition metals such as Fe, dependent on the impurity concentration. These impurities were magnetic and the host metal was not.(figure 1.3)

At the time, there was not any convincing theory to describe this minimum. The problem attracted many attentions. During 1950s, Friedel and coworkers tried to explain the trends in resistance when impurities varied across the transition elements.

The idea of 'virtual bound state' came out of their work. " states which are almost localized due to the resonant scattering at the impurity site" [19] are called virtual bound states. This concept was one of the significant steps toward an explanation of the resistance minimum.

Another important step, which in fact provided a derivation of the resistance minimum, was taken by J.Kondo in 1964. This derivation was an advance in the theory of magnetic impurities. Kondo assumed that there is a local magnetic moment associated with the impurity ion with spin S which is coupled via an exchange interaction with the conduction electrons. He showed, via third order perturbation theory in the coupling, that this interaction leads to a singular scattering of the conduction electrons near the Fermi level and a lnT contribution to the resistivity. [19]

Because of the lnT term, Kondo's derivation was not applicable when the zero temperature limit was taken. It turned out that Kondo's result is correct only above a certain temperature, which became known as the Kondo temperature T_K. This meant that a comprehensive theory was needed to explain the low temperature behaviour of the system giving the resistance minimum which has been called "Kondo problem" since then. In the 1960s P.W. Anderson introduced the theoretical framework for understanding the physics below T_k. His key idea was 'scaling' in the Kondo problem. Scaling idea assumes that low temperature properties of a system are adequately represented by a coarse grained model [19]. Such a scaling behaviour would imply a ground state in which a conduction electron is bound to the impurity in a singlet state. The calculations which used this key idea led to convincing results and explained the Kondo problem. In 1970s K.G. Wilson devised a non-perturbative method known as "numerical renormalization group" that overcame the shortcomings of standard perturbation theory and confirmed the scaling hypothesis.

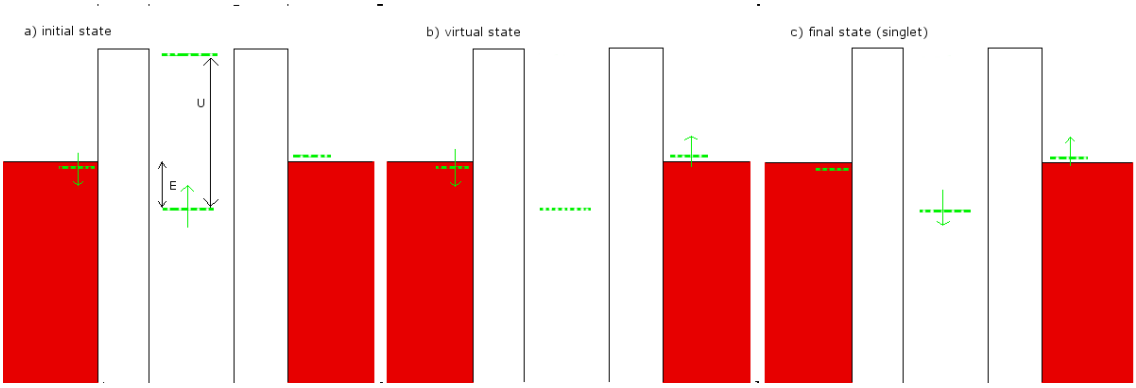

Figure 1.4: Anderson model of magnetic impurity [1]. (a) shows that energy level of impurity is below the Fermi level of the host metal ε_0 It costs U to add another electron to the impurity which is not favourable. (b) shows that the impurity electron tunnels out. (c) electron from host metal tunnels in. In this case spin of electron has flipped and a singlet has formed between electron in the impurity and the electron in "resonant level.

1.2.2 A Physical Description of the Kondo effect

As mentioned before, the anomalous behaviour in resistance or Kondo effect only happens to the magnetic impurities in the metals. It means that the spin plays an important role in this effect. Total spin of all the electrons in the impurity is nonzero and these electrons coexist with the mobile electrons in the metal which behave like a Fermi sea.[1] The simplest explanation of the effect is based on the Anderson model [1].(figure 1.4)

He assumes that the energy level of impurity is below the Fermi level of the host metal. This level is filled with an electron (magnetic impurity). Spin of electron has a definite value in the z direction. The electron can tunnel outside the impurity

to a virtual bound state close to the Fermi level of the host metal. Then another electron from the Fermi sea will be able to tunnel inside the impurity and during this process the spin can get flipped. It is favourable the electron which tunnels inside the impurity has spin in opposite direction respect to the electron in virtual bound state. As a result, hybridization happens and the electron inside the impurity and the electron in virtual bound state form a singlet. This process happens repeatedly and it results in appearance of an extra energy level at the Fermi surface called 'resonance level'.(figure 1.5)

Since the transport properties, such as the conductance, are determined by electrons with energies close to the Fermi level, the extra resonance level can dramatically change the conductance. The only requirement for the effect to occur is that the metal is cooled to a sufficiently low temperature below the Kondo temperature T_K.

1.2.3 Kondo effect in Quantum Dots

We discussed that quantum dots are like a quantum box. They can trap electrons in the box and also electrons can tunnel out. If we consider a quantum dot in contact with sources of electrons(leads), the situation resembles impurity in the metal. Consequently it is reasonable to expect to see the Kondo effect in quantum dot systems [25] [26]. As mentioned before, Kondo effect happens to the magnetic impurities so in order to see this effect in a quantum dot coupled to leads, the number of electrons on the dot has to be odd. [4] In this case phenomena such as spin flipping, singlet formation and virtual bound states happen in the case of quantum dots as well.

[4] recently the so called Kondo effect has been observed in dots with even number of electrons as well. This effect happens in Zeeman splitting regime and possibility of singlet and triplet states. [27] [24]

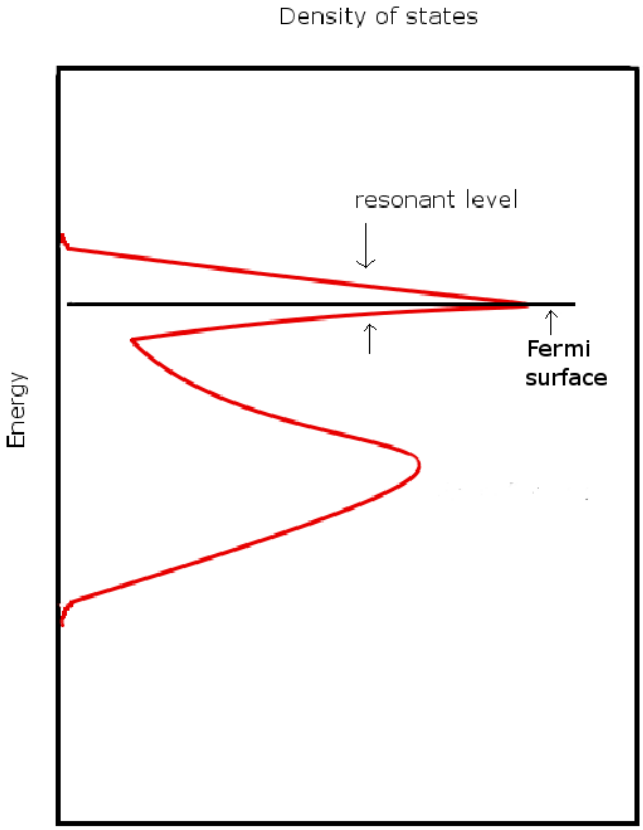

Figure 1.5: Density of states of impurity atom, the (extra) peak at the Fermi energy is due to the formation of the Kondo resonance.

In comparison with an impurity in a metal, the Kondo effect for quantum dots results in different outcome. This happens because of the different geometries of the two systems. Scattering of the plane waves(electron wavefunctions) from the impurity mixes the electron waves with different momenta and this increases the resistance in the case of the metal and impurity. But, for the quantum dots, because all electrons have to travel through the dot, Kondo resonance level makes it easier for electrons to pass through the dot. This increases the conductance. So the Kondo effect has the opposite behaviour in a quantum dot to that of a bulk metal. [1]

Therefore, at low enough temperature in a quantum dot system one can observe Kondo effect in a sense of a singlet formation (hybridization). Interesting situations can come about, when we have a system with multiple dots which are coupled to each other and coupled to the leads [28] [29] like our system (triple quantum dot system on the corners of an equilateral triangle). The coupling between dots and the coupling between dot and lead(which includes the Kondo effect at low enough temperature) can be adjusted. This can lead to a competition between a Kondo regime (singlet formation between lead and dot) and non-Kondo regime (singlet between dots). The dominant coupling can change the behaviour of the system and one can expect a case of quantum phase transition. This sort of competition between coupling constants which have caused quantum phase transition has been a rapidly developing area in condensed matter physics [21] [23] [16] [20].

1.3 Phase Transitions

1.3.1 General Concepts

Thermodynamic functions of a system provide results related to the bulk properties of that system. These macroscopic data can be tested in the laboratory. Statistical Mechanics provides a microscopic basis for thermodynamics. In terms of the behaviour

of thermodynamic functions, among systems to which the formalism of statistical mechanics has been applied, there are systems in which interparticle interactions can lead to analytic discontinuities or singularities in the thermodynamic functions of the given system. This happens for a small region of parameter space of the system and consequently various kinds of phase transitions occur. Condensation of gases, melting of solids, phenomena of ferromagnetism and superconductivity are examples of phase transitions.

In the case of phase transition, a large number of microscopic constituents of the system may exhibit a tendency of interacting with one another in rather strong, and cooperative fashion [30]. At a particular temperature called critical temperature, this cooperative behaviour becomes significant macroscopically and results in the analytic discontinuities and singularities.

We can define phase transitions mathematically as the regions in phase diagram where free energy is not analytic. The free energy analytic regions in the phase diagram are the phases of matter. As a result of this definition, and with considering the fact that free energy is continuous everywhere one can define various types of phase transitions. Generally, all phase transitions are either first order or continuous. First order phase transition happens when at least one first derivative of free energy is discontinuous across the phase boundaries. In continuous phase transition all first derivatives are continuous across the phase boundaries but some higher order derivatives of the free energy are discontinuous.

During 1930s L.D. Landau tried to offer a unified description of all continuous(second order) phase transitions based on the symmetries of the system. A symmetry, in general, imposes a type of order to the system which can be parameterized

by an 'order parameter'. The value of the order parameter changes when the related symmetry appears or disappears. When the temperature crosses a particular point called 'critical temperature', this value will change from nonzero to zero or vice versa. In fact with change of the symmetries of the system (caused by change of temperature), the phase of the matter will change. This brings up the fact that phases with different symmetries must be separated by a phase transition. This is the Landau's symmetry principle. The change of symmetry cannot be continuous, because a symmetry is either present or absent. This causes many of the analytic discontinuities and singularities during the phase transitions.

In fact, Landau hypothesized a kind of approach that could be applied to all phase transitions. All thermodynamic functions of a system can be computed by differentiating a functional L. L, Landau functional, depends on the coupling constants of the system and order parameter. It is related but not identical to the free energy. The state of the system will be specified by the absolute minimum of L with respect to the order parameter.

1.3.2 Universal Properties

Study of the behaviour of a given system in the neighbourhood of its critical point is a basic problem in the theory of phase transition because of the singularities of physical quantities pertaining to the system at the critical point [30]. It is common to express these singularities in terms of power laws characterized by a set of critical exponents which determine the qualitative nature of the critical behaviour of the system. Obtainment of close enough values for critical exponents in different systems raised the idea of universality of these critical exponents. Since these exponents represent qualitative nature of the phase transitions, it suggests that there are classes of

systems which despite their structural differences, display a critical behaviour that is qualitatively the same for all members of the class [30]. These classes are determined by the symmetry which is being broken when the phase transition happens. They can be categorized by d, dimensionality of the space in which the system is embedded, and n, the number of components of the order parameter of the system. Because Landau's theory (in the way formulated by himself) is mean field theory, fluctuation effects are not included in this theory. Further calculations and experiments showed that fluctuation effects and as a result range of microscopic interactions play an important role in phase transitions. It seemed that a more comprehensive theory is needed to provide a more satisfactory picture of the critical phenomena than Landau's theory.

Attempts to generalize Landau's theory led to the 'scaling hypothesis' for the thermodynamic functions. The universal expression of Landau's functional was one of the most important outcomes of the scaling hypothesis:

$$L(t,h) \approx F\,|t|^{2-\alpha}\, f(\frac{Gh}{|t|^{\Delta}}) \tag{1.3}$$

in this relation α and Δ are universal exponents common to all systems in a given universality class. $f(x)$ is a universal function which is expected to have different branches for $t > 0$ and $t < 0$ where t is $\frac{T-T_C}{T_C}$. h is the ordering external field, F and G are nonuniversal parameters characteristic of the particular system under consideration [30]. The especial property of this expression is the dimensionless argument of universal function f and this argument provides a scale formed of system's variables. Scaling hypothesis indicates that for each universality class, one can find a universal function f with dimensionless argument. The scaling approach took the subject of phase transition far beyond mean-field theory. This idea emerged independently from three different sources [5] and Kadanoff(1966) suggested a scaling hypothesis [30].

[5] Widom(1965), Domb and Hunter (1965), Patashinski and Pokrovskii (1966)

It is a legitimate question to ask why a large variety of systems differing widely in their structures should belong to a single universality class and hence have common critical exponents and common scaling functions. The answer is that the structural details at the local level gets irrelevant when correlations between the microscopic constituents of system become large enough to prevail over macroscopic distances at critical temperature. This is the strong and cooperative behaviour of constituents mentioned earlier. As system approaches to its critical point its correlation length becomes exceedingly large and as a consequence system sensitivity to a length transformation becomes exceedingly diminished [30]. In other word, the system loses its reference to a length scale. This idea was first propounded by Kadanoff (1966). Consideration of correlations and correlation functions among microscopic constituents of the system led to a formulation which was similar to scaling hypothesis. Despite the convincing argument of Kadanoff, his approach did not provide a systematic means of deriving the critical exponents or of constructing the scaling functions which appear in the formulation. These deficiencies were remedied after K.G. Wilson introduced a new frame work of understanding to the field theory.(concept of renormalization group)

1.3.3 Quantum Phase Transitions

One of the most interesting subjects related to the phase transitions which have attracted lots of attentions in recent years is 'quantum phase transition'. One can describe the quantum phase transition as a phase transition at absolute zero of temperature which a quantum system can undergo as a parameter entering its Hamiltonian is varied. According to this definition there is a key point about quantum phase transitions. They happen only at absolute zero of temperature. So, all phase transitions that happen at finite temperature are classical phase transitions. This does not mean

that quantum mechanical effects are not important in classical phase transitions; superfluidity and superconductivity are categorized as classical phase transitions. But quantum fluctuations, near the critical point, for these systems are not long range and classical thermal fluctuations control all the critical behaviour of the correlations at long distances [31] and as mentioned earlier, these correlations determine the characteristic of a phase transition.

Because quantum phase transitions happen at absolute zero of temperature, thermal fluctuations do not exist in these phenomena. Consequently crossing the phase boundaries at $T = 0$ occurs differently. In this condition, the system is in its ground state and a parameter in the Hamiltonian of the system plays the role of temperature. If the value of this parameter crosses a certain point, the system will cross the phase boundaries. This means the ground state of the system changes by tuning a parameter in the Hamiltonian and a quantum phase transition takes place.

In order to make the situation clearer, we consider a Hamiltonian $H(g)$, whose degrees of freedom reside on the sites of a lattice and which varies as a function of dimensionless coupling g [32]. As a result the eigenvalues and eigenfunctions of H will be functions of g. If g couples only to a conserved quantity say $H(g) = H_0 + gH_1$ and $[H_0, H_1] = 0$ then eigenfunctions will be independent of g and only eigenvalues vary with g. There is a chance that a level crossing happens where an excited state becomes the ground state at $g = g_C$. This level crossing changes the 'phase of the system' via changing the ground state at $T = 0$ when the value of g crosses g_C and "quantum phase transition" happens. This (level crossing) corresponds to first order quantum phase transition. On the other hand, in the case of quantum continuous phase transition, the actual level-crossing does not happen. More particularly, in this case we are dealing with an "avoided level-crossing" between the ground and an

excited state. This avoided level-crossing can become progressively sharper as the lattice size increase, leading to a nonanalyticity at $g = g_C$ in the infinite lattice limit.

Correlation functions categorize phase transitions in universal classes and they represent cooperative behaviour of the constituents. Quantum and classical phase transitions behave similarly close to their critical point in this manner. As an example for quantum phase transitions, the critical behaviour of the energy scale fluctuations (above the ground state) of the system is described by a power law with universal critical exponents:

$$\Delta \approx J \left| g - g_C \right|^{z\nu} \tag{1.4}$$

J is a non-universal constant of proportionality related to the microscopic structures of the system. Δ vanishes as g approaches to g_C according to the above power law. This means the time scale diverges according to Heisenberg uncertainty principle.

Divergent correlation length in quantum phase transitions is another example. This length characteristic behaves as

$$\xi^{-1} \approx \Lambda \left| g - g_C \right|^{\nu} \tag{1.5}$$

where Λ is an inverse length scale (a 'momentum cutoff') and ν is a universal critical exponent. ξ can be the length scale determining the exponential decay of equal-time correlations in the ground state or the length scale at which some characteristic cross-over occurs to the correlations at the longest distance [32].

The physics underlying quantum phase transitions is quite complex and in many cases not completely understood [32]. Different theoretical models have been used to analyze the physical properties of quantum phase transitions. The central importance of these models turns out to be that quantum phase transitions in these models in d dimensions are intimately connected to certain well-studied finite-temperature (classical) Phase transitions in $D = d + \delta$ dimensions (mapping to classical models).

δ can be greater than or equal to one depending on the system under study. Then the sophisticated technology of analyzing the classical model can be transferred to quantum problems. If we consider the case of $\delta = 1$, the extra dimension comes from the method of calculation of partition function via path integral in quantum model. With consideration of $\beta = \frac{1}{k_B T}$ as imaginary time, the partition function of the quantum system can be calculated as a path integral. In analogy with a classical system the imaginary time will be added to spatial dimensions and the classical counterpart will have one extra "spatial dimension" [31]. Generally the resulting classical phase transition problems are not very simple and a direct treatment of quantum problems is certainly needed [32].

1.4 In this Thesis

In previous sections of the introductory, we reviewed quantum dots, Kondo effect, phase transition and quantum phase transition. We saw, because physical characteristics of systems composed of quantum dots plus metal leads and metal with impurities are similar, Kondo effect can occur in quantum dot systems. We also concluded that, in a system with multiple coupled quantum dots, a competition can happen between a Kondo and non-Kondo regimes by adjusting the coupling constants and this results in a quantum phase transition.

Probe of quantum phase transition in systems composed of quantum dots, have recently been a growing subject in both theoretical and experimental areas.[21] [23] [16] [20] are examples of recent experimental and theoretical investigations in this subject. Among theoretical works, systems composed of two coupled dots have been considered. Common techniques have been used in these theoretical works to get an effective Hamiltonian of the system. In this thesis we consider a triple quantum dot system. We use slave-boson mean field theory to obtain an effective Hamiltonian and by solving mean field equations we probe quantum phase transition(chapter two).

By utilizing "scattering formalism" in chapter 3 we seek consequences of this phase transition on transport. In particular, we introduce the low energy Hamiltonian of our system. The coupling ratio $\frac{J}{J_K}$ plays the role of g and brings up the possibility of quantum phase transition in our system.

Chapter 2

Effective Low Energy Hamiltonian and Analysis

In this chapter, Hamiltonian of the system under study will be introduced, triple quantum dot system which the dots are sitting on the corners of an equilateral triangle. Each dot is coupled to a lead and to two other dots. We try to calculate the effective Hamiltonian by integrating out the high energy degrees of freedom and by using slave-boson mean field theory.

2.1 Low Energy Hamiltonian

Microscopic Hamiltonian of the three quantum dots coupled to each other and coupled to three leads can be written as the following. (In the upcoming relations Einstein summation convention is considered over the index s and s'.)

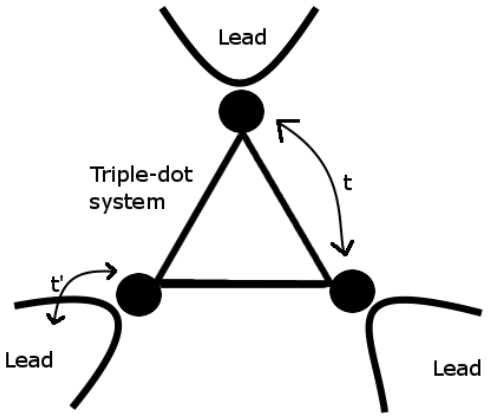

Figure 2.1: Figure of our system, the bent lines represent leads, and black circles represent dots. t and t' are constants for electrons hopping from"dot to dot" and from "lead to dot or dot to lead".

$$H_{dot} = \varepsilon_0 \sum_l c_{ls}^\dagger c_{ls} + U \sum_l n_{l\uparrow} n_{l\downarrow} + V \sum_l n_{l+1} n_l \tag{2.1}$$

The Hamiltonian which we use to describe the leads is the following

$$H_{leads} = \sum_l \sum_p \varepsilon_p c_{lps}^\dagger c_{lps} \tag{2.2}$$

$$H_{perturbative} = -t \sum_l (c_{l+1s}^\dagger c_{ls} + c_{ls}^\dagger c_{l+1s}) + t' \sum_l \psi_{ls}^\dagger(0) c_{ls} + c_{ls}^\dagger \psi_{ls}(0) \tag{2.3}$$

where

$$\psi_{ls}(\vec{r}) = \frac{1}{\sqrt{V}} \sum_p e^{i\vec{p}\cdot\vec{r}} c_{pls} \tag{2.4}$$

consequently, the Hamiltonian will be

$$H_{microscopic} = H_{dot} + H_{leads} + H_{pertubative} \tag{2.5}$$

2.1.1 From Anderson to Kondo

Equation 2.5, the microscopic Hamiltonian of our system, is an Anderson model Hamiltonian. As we mentioned before, we are interested in low energy degrees of freedom. So to continue, we need to integrate out the high energy degrees of freedom of the Anderson Hamiltonian. This yields to an effective Kondo Hamiltonian. In other words, this process is a projection to the low energy space. To see how one can get the effective Kondo Hamiltonian by starting from Anderson Hamiltonian, we describe simple case of one impurity Anderson model. The Hamiltonian for this system is

$$\begin{aligned} H &= \sum_{\sigma} \varepsilon_d n_{d\sigma} + U n_{d\uparrow} n_{d\downarrow} \\ &\quad + \sum_{\vec{k}\sigma} \varepsilon_{\vec{k}} c^{\dagger}_{\vec{k}\sigma} c_{\vec{k}\sigma} \\ &\quad + \sum_{\vec{k}\sigma} (V_{\vec{k}} c^{\dagger}_{d\sigma} c_{\vec{k}\sigma} + V^{*}_{\vec{k}} c^{\dagger}_{\vec{k}\sigma} c_{d\sigma}) \end{aligned} \tag{2.6}$$

which is one of the simplest forms (only spin degeneracy for impurity, basically one state available for electrons on the impurity without spin consideration). The third term of this Hamiltonian describes creation and annihilation from impurity to host metal and vice versa. To get some insight, if we consider $V_{\vec{k}} = 0$, we see that there are three possible energy configurations for the impurity state: (a) zero occupation with a total energy $E_0 = 0$; (b)single occupation by a spin σ with a total energy $E_{1\sigma} = \varepsilon_d$ where $\sigma = \uparrow, \downarrow$; (c) double occupation with a total energy $E_2 = 2\varepsilon_d + U$. (see figure 1.4)

As we mentioned in introductory chapter, Anderson assumed that the energy level of impurity is below the Fermi energy of the host metal. This favors the single

occupation as a ground state for the situation (impurity and host metal). Now if we turn on $V_{\vec{k}}$ which means $V_{\vec{k}} \neq 0$ the local impurity state and conduction electrons from host metal will be mixed. If we consider the regime where $V_{\vec{k}}$ is sufficiently small we can apply perturbation theory.

Our goal is to solve the equation $H\psi = E\psi$ where H is the equation 2.6. We choose the eigenstates of Hamiltonian when we assumed $V_{\vec{k}} = 0$ as our basis and we write the Schrodinger equation as

$$\begin{pmatrix} H_{00} & H_{01} & H_{02} \\ H_{10} & H_{11} & H_{12} \\ H_{20} & H_{21} & H_{22} \end{pmatrix} \begin{pmatrix} \psi_0 \\ \psi_1 \\ \psi_2 \end{pmatrix} = E \begin{pmatrix} \psi_0 \\ \psi_1 \\ \psi_2 \end{pmatrix}$$

where $H_{nn'} = P_n H P_{n'}$ and P_n is a projection operator on the "subspace with impurity occupation n. As there is no term in the equation 2.6 in which two electrons are simultaneously removed from or added to th impurity $H_{02} = H_{20} = 0$. The other off diagonal matrix elements of H arise from hybridization terms.

We are interested in a singly occupied state in order to have a magnetic impurity.(As we said we are looking for a effective Kondo Hamiltonian) So we eliminate ψ_0 and ψ_2 in the equation which we get after performing matrix multiplication for ψ_1.(equation 2.7)

$$\left[H_{11} + H_{12}(E - H_{22})^{-1}H_{21} + H_{10}(E - H_{00})^{-1}H_{01}\right]\psi_1 = E\psi_1 \tag{2.7}$$

By doing the projections $H_{nn'} = P_n H P_{n'}$ we get each matrix elements. Substituting the results of projection into equation 2.7 and keeping terms to the lowest order in $V_{\vec{k}}$ will lead to the effective Kondo Hamiltonian.

Same procedure is applicable to our system, but with more complicated algebra. Here we present the result of this projection for our Hamiltonian from reference [33].

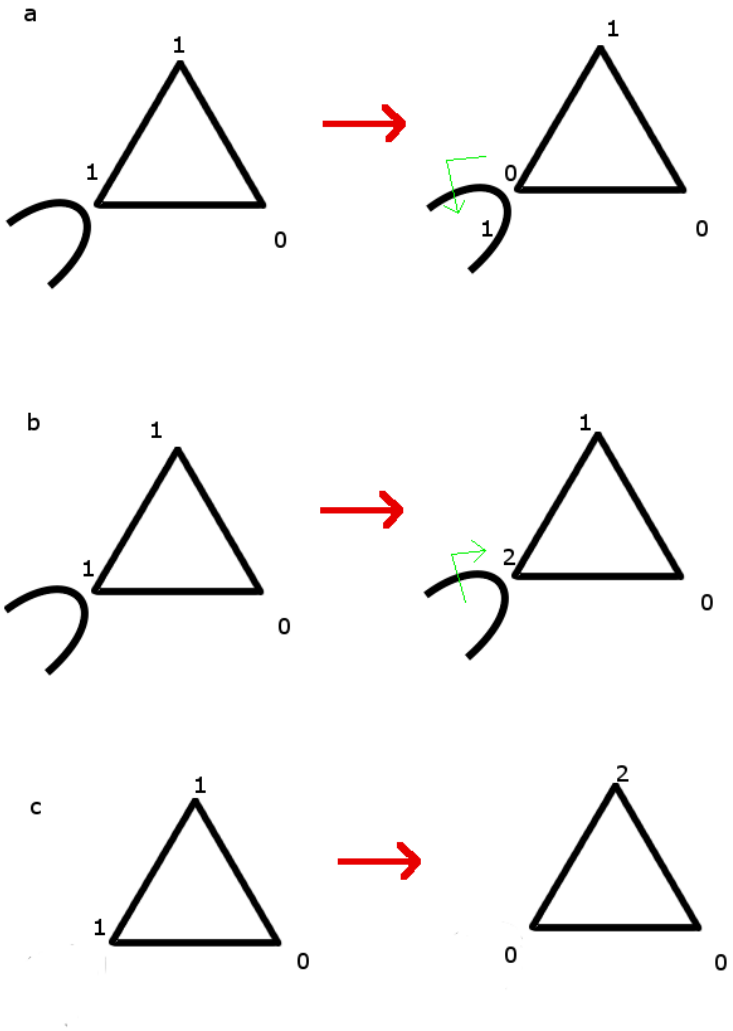

Figure 2.2: examples of high energy configurations which has been integrated out. In each corner (which practically is a quantum dot) the number of electrons has been shown.

$$
\begin{aligned}
H_{lowenergy} &= -t\sum_{l} c^{\dagger}_{l+1s}c_{ls} + c^{\dagger}_{ls}c_{l+1s} \\
&+ J\sum_{l} \vec{S}_{l+1}\cdot\vec{S}_{l} - \frac{1}{4}n_{l+1}n_{l} \\
&+ J'\sum_{l} (c^{\dagger}_{l+1s}c_{ls'} + c^{\dagger}_{ls}c_{l+1s'})\vec{S}_{ss'}\cdot\vec{S}_{l+2} - \frac{1}{4}(c^{\dagger}_{l+1s}c_{ls} + c^{\dagger}_{ls}c_{l+1s})n_{l+2} \\
&- \frac{J_K}{2}\sum_{l} (\psi^{\dagger}_{ls}(0)c_{ls})(c^{\dagger}_{ls}\psi_{ls}(0)) \\
&- \frac{J'_K}{2}\sum_{i<j} (\psi^{\dagger}_{is}(0)c_{is})(c^{\dagger}_{js}\psi_{js}(0)) + (\psi^{\dagger}_{js}(0)c_{js})(c^{\dagger}_{is}\psi_{is}(0)) \qquad (2.8)
\end{aligned}
$$

In this Hamiltonian first term represents hopping without any spin flipping, second term represents interactions between two electrons and their spins on two different corners, third term describes correlated hopping during which spins will flip, fourth and fifth terms come from the Kondo effect with the difference we can see in fig.2.3(operators f and b will be described later)

In our problem we only consider two electrons on our triple-dot system. So we have always one dot free. This enforces the following constraints

$$
\begin{aligned}
c^{\dagger}_{ls}c_{ls} &\leq 1 \qquad (2.9) \\
\sum_{l} c^{\dagger}_{ls}c_{ls} &= 2 \qquad (2.10)
\end{aligned}
$$

The goal, from this point, is to simplify 2.8 and 2.9 in order to get proper form of effective Hamiltonian. To do this we rewrite the low energy Hamiltonian in a way that makes our analysis easier.

2.1.2 Slave-boson Analysis

Because equation 2.8 and in particular equation 2.9 is difficult to deal with, we facilitate the analysis by introducing new fermion and boson operators to describe the

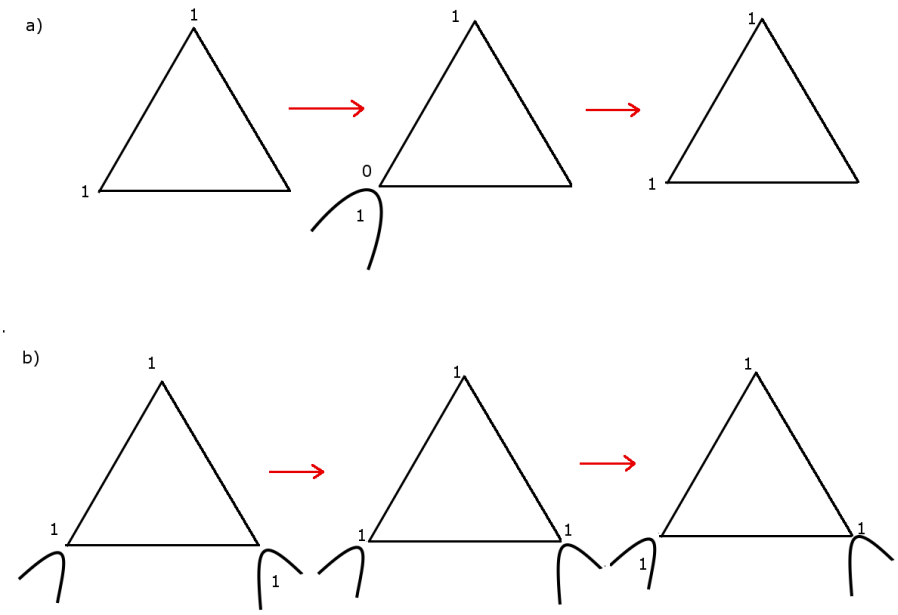

Figure 2.3: (a) shows processes which fourth term of low energy Hamiltonian (2.8 represents, Kondo effect, one electron from a quantum dot tunnels out and another electron tunnels in and both happens at the same corner. Spin flip can also happen. (b) represents the fifth term. It is basically the same process as (a) but tunnelling in and tunnelling out happens at different corners.

creation and annihilation of electrons in dots. We consider f operators associated with electrons and b operators which are spinless Boson operators, representing the empty dot in triple-dot system. We can express the creation and annihilation operators $c_{ls}^{\dagger}$ and c_{ls} in terms of the new ones $f^{\dagger}, f, b^{\dagger}, b$ as the following

$$c_{ls} = f_{ls} b_{l}^{\dagger} \tag{2.11}$$

According to the above expression annihilation of one electron on a dot is accompanied by creation of a "hole" (empty dot) at the same spot. This means the creation of a spinfull fermion (the electron) comes along with annihilation of a spinless boson (empty spot). So this type of analysis is called "slave-boson formalism". The relation for $c_{ls}^{\dagger}$ is simply the complex conjugate of the above relation. By this definition (2.11) our constraints will change into a simpler form

$$b_{l}^{\dagger} b_{l} + f_{ls}^{\dagger} f_{ls} = 1 \tag{2.12}$$

$$\sum_{l} f_{ls}^{\dagger} f_{ls} = 2 \tag{2.13}$$

$$\tag{2.14}$$

We also need to specify spin operators which appear in the low energy Hamiltonian. Because we have assigned new spinfull fermion and spinless boson operators to each site at triangle, spin operators can be expressed as the following

$$\vec{S}_{l} = \vec{S}_{ss'} f_{ls}^{\dagger} f_{ls'} \tag{2.15}$$

The above expression is related to an electron's spin on the l_{th} site so no hole will be created on that site while an electron is present and its spin is being measured.

To continue insert $f^{\dagger}, f, b^{\dagger}, b$ in our low energy Hamiltonian

$$
\begin{aligned}
H_{lowenergy} &= -t\sum_{l} b_{l+1}f^{\dagger}_{l+1s}f_{ls}b^{\dagger}_{l} + b_{l}f^{\dagger}_{ls}f_{l+1s}b^{\dagger}_{l+1} \\
&+ J\sum_{l}(\vec{S}_{ss'}f^{\dagger}_{l+1s}f_{l+1s'})\cdot(\vec{S}_{tt'}f^{\dagger}_{lt}f_{lt'}) - \frac{1}{4}(f^{\dagger}_{l+1s}f_{l+1s})(f^{\dagger}_{lt}f_{lt}) \\
&+ J'\sum_{l}(b_{l+1}f^{\dagger}_{l+1s}f_{ls'}b^{\dagger}_{l} + b_{l}f^{\dagger}_{ls}f_{l+1s'}b_{l+1})\vec{S}_{ss'}\cdot\vec{S}_{tt'}f^{\dagger}_{l+2t}f_{l+2t'} \\
&- J'\sum_{l}\frac{1}{4}(b_{l+1}f^{\dagger}_{l+1s}f_{ls}b_{l} + b_{l}f^{\dagger}_{ls}f_{l+1s}b_{l+1})f^{\dagger}_{l+2t}f_{l+2t} \\
&- \frac{J_K}{2}\sum_{l}(\psi^{\dagger}_{ls}(0)f_{ls})(f^{\dagger}_{ls}\psi_{ls}(0)) \\
&- \frac{J'_K}{2}\sum_{i<j}(\psi^{\dagger}_{is}(0)f_{is}b^{\dagger}_{i})(b_{j}f^{\dagger}_{js}\psi_{js}(0)) + (\psi^{\dagger}_{js}(0)f_{js}b^{\dagger}_{j})(b_{i}f^{\dagger}_{is}\psi_{is}(0))
\end{aligned}
\tag{2.16}
$$

where n_l has been replaced by $f^{\dagger}_{ls}f_{ls}$.(Same argument as spin operator applies in this situation.)

[Note: Same fermion f and boson b operators has been used in the fourth and fifth term of equation 2.8. The fourth term represents forming of a singlet which one electron in the dot is coupled to an electron in the lead. This leaves no empty space, and as a result there is no b operator in the fourth term.]

Another step towards the effective Hamiltonian is to impose the constraints 2.12 to equation 2.16. The application of constraints will be done using auxiliary fields (Lagrange multipliers) λ_1 and λ_2 in the form of Delta function

$$
\delta(f^{\dagger}_{ls}f_{ls} + b^{\dagger}_{l}b_{l} - 1) = \frac{1}{2\pi}\int_{-\infty}^{\infty} d\lambda_1 e^{i\lambda_1(f^{\dagger}_{ls}f_{ls} + b^{\dagger}_{l}b_{l} - 1)} \tag{2.17}
$$

$$
\delta(\sum_{l} f^{\dagger}_{ls}f_{ls} - 2) = \frac{1}{2\pi}\int_{-\infty}^{\infty} d\lambda_2 e^{i\lambda_2(\sum_{l} f^{\dagger}_{ls}f_{ls} - 2)} \tag{2.18}
$$

We apply the above forms of constraints to the "partition function" of our system and we get a rather complete expression for the effective Hamiltonian.

$$Z = \frac{1}{(2\pi)^2}\int \quad D\lambda_1 D\lambda_2 \prod_{ls} \mathrm{D}\psi^\dagger_{ls}\mathrm{D}\psi_{ls}\mathrm{D}f^\dagger_{ls}\mathrm{D}f_{ls}\mathrm{D}b^\dagger_l\mathrm{D}b_l \times e^{-\int_0^\beta d\tau H_{eff}} \times e^{-\int_0^\beta d\tau \sum_{ls}(b^\dagger_l\partial_\tau b_l + f^\dagger_{ls}\partial_\tau f_{ls} + \psi^\dagger_{ls}\partial_\tau\psi_{ls})} \tag{2.19}$$

Where

$$H_{eff} = (H_{lowenergy} + H_{leads} + i\lambda_2(\sum_l f^\dagger_{ls}f_{ls} - 2) + i\lambda_1(f^\dagger_{ls}f_{ls} + b^\dagger_l b_l - 1)) \tag{2.20}$$

and $\tau = it$ is the imaginary time. The above representation of Z is a functional integral representation over Bose and Fermi field as well as λ_i. τ is imaginary time and is

To get a simplified expression for the low energy Hamiltonian we apply the following relations to the terms including $\vec{S}_{ss'} \cdot \vec{S}_{tt'}$

$$\vec{S}_{ss'} \cdot \vec{S}_{tt'} = \frac{1}{2}(S^+_{ss'}S^-_{tt'} + S^-_{ss'}S^+_{tt'}) + S^z_{ss'}S^z_{tt'} \tag{2.21}$$

$S^\pm = S^x \pm iS^y$, $S^{x,y,z}$ are spin-$\frac{1}{2}$ operators and s, s', t, t' take the spin values $\uparrow$ and $\downarrow$. Using this relation and after some simple algebra we can get

$$\begin{aligned}(\vec{S}_{ss'}f^\dagger_{l+1s}f_{l+1s'}) \cdot (\vec{S}_{tt'}f^\dagger_{lt}f_{lt'}) - \frac{1}{4}(f^\dagger_{l+1s}f_{l+1s})(f^\dagger_{lt}f_{lt}) \;&=\; -\frac{1}{2}(f^\dagger_{l+1s}f_{ls})(f^\dagger_{lt}f_{l+1t}) \\ &\quad -\frac{1}{2}(f^\dagger_{l+1s}f_{l+1s})(1 - f^\dagger_{lt}f_{lt})\end{aligned} \tag{2.22}$$

as second term of equation2.16. Third term of equation 2.16(low energy Hamiltonian) will be the following after substitution of spin operators and mean fields

$$
\begin{aligned}
&-\frac{1}{2}(b_{l+1}f^{\dagger}_{l+1s}f_{ls}b^{\dagger}_{l}+b_{l}f^{\dagger}_{ls}f_{l+1s}b^{\dagger}_{l+1})(f^{\dagger}_{l+2t}f_{l+2t})\\
&-\frac{1}{2}(b_{l}f^{\dagger}_{l\uparrow}f_{l+2\uparrow}+b_{l+1}f^{\dagger}_{l+1\downarrow}f_{l+2\downarrow})(f^{\dagger}_{l+2\uparrow}f_{l\uparrow}b^{\dagger}_{l}+f^{\dagger}_{l+2\downarrow}f_{l+1\downarrow}b^{\dagger}_{l+1})\\
&+\frac{1}{2}b_{l}f^{\dagger}_{l\uparrow}f_{l+2\uparrow}f^{\dagger}_{l+2\uparrow}f_{l\uparrow}b^{\dagger}_{l}\\
&+\frac{1}{2}b_{l+1}f^{\dagger}_{l+1\downarrow}f_{l+2\downarrow}f^{\dagger}_{l+2\downarrow}f_{l+1\downarrow}b^{\dagger}_{l+1}\\
&-\frac{1}{2}(b_{l}f^{\dagger}_{l\downarrow}f_{l+2\downarrow}+b_{l+1}f^{\dagger}_{l+1\uparrow}f_{l+2\uparrow})(f^{\dagger}_{l+2\downarrow}f_{l\downarrow}b^{\dagger}_{l}+f^{\dagger}_{l+2\uparrow}f_{l+1\uparrow}b^{\dagger}_{l+1})\\
&+\frac{1}{2}b_{l}f^{\dagger}_{l\downarrow}f_{l+2\downarrow}f^{\dagger}_{l+2\downarrow}f_{l\downarrow}b^{\dagger}_{l}\\
&+\frac{1}{2}b_{l+1}f^{\dagger}_{l+1\uparrow}f_{l+2\uparrow}f^{\dagger}_{l+2\uparrow}f_{l+1\uparrow}b^{\dagger}_{l+1}\\
&+\frac{1}{4}(b_{l}f^{\dagger}_{l\uparrow}f_{l+1\uparrow}b^{\dagger}_{l+1}+b_{l+1}f^{\dagger}_{l+1\uparrow}f_{l\uparrow}b^{\dagger}_{l}+f^{\dagger}_{l+2\uparrow}f_{l+2\uparrow})^{2}\\
&-\frac{1}{4}(b_{l}f^{\dagger}_{l\uparrow}f_{l+1\uparrow}b^{\dagger}_{l+1}+b_{l+1}f^{\dagger}_{l+1\uparrow}f_{l\uparrow}b^{\dagger}_{l})^{2}\\
&-\frac{1}{4}(f^{\dagger}_{l+2\uparrow}f_{l+2\uparrow})^{2}\\
&+\frac{1}{4}(b_{l}f^{\dagger}_{l\downarrow}f_{l+1\downarrow}b^{\dagger}_{l+1}+b_{l+1}f^{\dagger}_{l+1\downarrow}f_{l\downarrow}b_{l}+f^{\dagger}_{l+2\downarrow}f_{l+2\downarrow})^{2}\\
&-\frac{1}{4}(b_{l}f^{\dagger}_{l\downarrow}f_{l+1\downarrow}b^{\dagger}_{l+1}+b_{l+1}f^{\dagger}_{l+1\downarrow}f_{l\downarrow}b_{l})^{2}\\
&-\frac{1}{4}(f^{\dagger}_{l+2\downarrow}f_{l+2\downarrow})^{2}
\end{aligned}
\tag{2.23}
$$

Equations 2.22 and 2.23 and fourth and fifth term of equation 2.16 include operators of the form $AA^{\dagger}$ which $A = A^{\dagger}$ for some of them (A is just a typical operator and can be either $b_i f^{\dagger}_{is} f_{js} b^{\dagger}_{j}$ or $\psi^{\dagger}_{is} f_{js} b^{\dagger}_{j}$ in our case). We use the 'undoing Gaussian integral' trick or Hubbard-Stratonovich (HS) transformation to deal with these terms. This is another step to get a more simplified Hamiltonian to continue.

$$
\int \prod_{i}^{N} dz^{*}_{i} dz_{i} e^{-\vec{z}^{\dagger} M \vec{z} - \vec{J}^{\dagger}\cdot\vec{z} - \vec{z}^{\dagger}\vec{J}} = \frac{(2\pi i)^{N}}{detM} e^{\vec{J}^{\dagger} M^{-1} \vec{J}} \tag{2.24}
$$

This equation is HS transformation. We apply this transformation for all terms of the form $AA^{\dagger}$ in equations 2.22 and 2.23 and fourth and fifth term of equation

2.16. As a result of this transformation, auxiliary fields z_i will be entered in our Hamiltonian and these auxiliary fields have to be determined in the next section. We present the result of this transformation in appendix A. Basically it is a simple algebraic rewriting of equations 2.22 and 2.23 and fourth and fifth term of equation 2.16. As we can see in equation 2.24 the auxiliary field $\vec{z}$ is generally complex. In our problem because of the symmetries of our Hamiltonian, we can consider real auxiliary fields (see Appendix B).

2.2 Mean-Field Theory

The next step is to analyze the Hamiltonian which we obtained by rewriting the low energy Hamiltonian in the previous section. Consequently the partition function of our system will be

$$\begin{aligned} Z = \frac{1}{(2\pi)^2}\int \quad & D\lambda_1 D\lambda_2 \prod_i^N Dz_i \prod_{ls} \mathrm{D}\psi_{ls}^\dagger \mathrm{D}\psi_{ls} \mathrm{D}f_{ls}^\dagger \mathrm{D}f_{ls} \mathrm{D}b_l^\dagger \mathrm{D}b_l \\ & \times e^{-\int_0^\beta d\tau H_{eff}(z_i, b_l, b_l^\dagger, f_{ls}, f_{ls}^\dagger, \psi_{ls}, \psi_{ls}^\dagger)} \\ & \times e^{-\int_0^\beta d\tau \sum_{ls}(b_l^\dagger \partial_\tau b_l + f_{ls}^\dagger \partial_\tau f_{ls} + \psi_{ls}^\dagger \partial_\tau \psi_{ls})} \end{aligned} \tag{2.25}$$

As we can see, equation 2.25 is the functional integral representation of the partition function Z and calculating this integrals is very complicated. We approximate the evaluation of integrals using a saddle point evaluation (the simplest approximation of functional integral which is replacement of integrand by its maximum value). In order to do this replacement we minimize $< H_{eff} >$ with respect to all auxiliary fields, and replace them with the value we get from this procedure. This corresponds to a mean-field type of approximation.

As we described above mean field theory imposes (thermal)average values of the auxiliary fields ($< H_{eff} >$). So it is a powerful tool in exploring the qualitative phase

structure of a system [34]. It is the first method to try in new situations (zeroth approximation). The mean-field approximation is also very crude. In some cases it has led to incorrect quantitative results. The reason is since mean field theory applies average values, it does not take into account the fluctuations about those "mean fields".

In the case of our problem, because we are interested in $T = 0$ regime, those fluctuations about mean values are highly diminished. So we expect to get reasonably reliable results using mean-field theory in this regime. As mentioned above, the qualitative picture provided by mean-field theory is powerful to seek the case of quantum phase transition. To probe the fluctuations and their importance in this case, one needs to employ other tools like renormalization group which can be the subject of future projects.

2.2.1 Applying Mean-Fields

In the mean field approximation on equation 2.16 we replace the Bose operators $b_l^\dagger$ and b_l by their expectation values $b_l^\dagger \rightarrow < b_l^\dagger >= b$ and $b_l \rightarrow < b_l >= b$. After applying the HS transformation which is basically transforming two body interaction term to a term which one body is interacting with a mean field, we can find all our auxiliary fields by minimizing the effective Hamiltonian respect to these "mean fields" $\frac{\partial < H_{eff} >}{\partial x_i} = 0$ where x_i represents our auxiliary fields including λ_i, b, z_i. z_i are auxiliary fields entered by HS transformation (appendix 1). Because of the structure of the terms which HS transformation has been applied to (either $f_{is}^\dagger f_{js}$ or $\psi_{is}^\dagger f_{js}$) and because of the symmetries of our system (see Appendix 2) only three real auxiliary fields beside λ_i, b are needed. The followings are the mean field equations which we get by minimizing respect to z_i and which have to be determined "self-consistently"(next section)

$$\begin{aligned} n &= < f^{\dagger}_{l\sigma} f_{l\sigma} > \\ \eta &= < f^{\dagger}_{l+1\sigma} f_{l\sigma} > \\ \chi &= < \psi^{\dagger}_{l\sigma} f_{l\sigma} > \end{aligned} \tag{2.26}$$

Where σ can be either $\uparrow$ or $\downarrow$.

Minimizing respect to λ_1 and λ_2 results in the constraints in the following form

$$\begin{aligned} < f^{\dagger}_{ls} f_{ls} > + b^2 - 1 &= 0 \\ \sum_l < f^{\dagger}_{ls} f_{ls} > - 2 &= 0 \end{aligned} \tag{2.27}$$

Solving these two equations gives us $n = b^2 = \frac{1}{3}$ and also we can substitute $f^{\dagger}_{ls} f_{ls}$ with $1 - b^2 = \frac{2}{3}$ (This substitution comes in handy after HS transformation and in terms like first term of equation 2.23.)

After applying the above transformations and substitutions we get our final expression for the effective Hamiltonian

$$\begin{aligned} H_{eff} &= t_0 \sum_l (f^{\dagger}_{l+1s} f_{ls} + f^{\dagger}_{ls} f_{l+1s}) \\ &\quad + \mu_0 \sum_l f^{\dagger}_{ls} f_{ls} + V_0 \sum_l (\psi^{\dagger}_{ls}(0) f_{ls} + f^{\dagger}_{ls} \psi_{ls}(0)) \\ &\quad + constant + H_{leads} \end{aligned} \tag{2.28}$$

where the constant can be eliminated by moving the reference point of energy and μ_0, V_0 and t_0 are the followings

$$\begin{aligned} t_0 &= \frac{1}{6} J' n + (-J - \frac{J'}{3})\eta - \frac{1}{3}(t + \frac{J'}{3}) \\ \mu_0 &= \frac{J'}{3}\eta \\ V_0 &= -\chi(J_K + \frac{2J'_K}{3}) \end{aligned} \tag{2.29}$$

It turns out minimization of effective Hamiltonian respect to b^2 gives us real value for $i(\lambda_1 + \lambda_2)$ so we have a real μ. μ is the chemical potential and the coefficient of $f_{ls}^\dagger f_{ls}$, we can shift the value of the μ by $i(\lambda_1 + \lambda_2)$ and define $\mu_0 = \mu - i(\lambda_1 + \lambda_2)$. As a result these Lagrange multipliers do not appear in the expression of μ_0.

2.2.2 Calculating the Mean-Field Variables

As mentioned in the previous section, to get the effective Hamiltonian thoroughly we need to solve the mean field equations self-consistently. The first step of solving equation 2.26 is to find a proper expression for the expectation values appearing in these equations. To do so we use the "spectral density" representation (related calculation of the first equation of 2.30 can be found in appendix C)

$$\begin{aligned} < f_{l\sigma}^\dagger f_{l\sigma} > &= \frac{1}{2\pi}\int_{-\infty}^{\infty} d\omega f(\omega) A(\omega) \\ A(\omega) &= -2Im(G(\omega)) \\ G(\omega) &= \int_{-\infty}^{\infty} dt e^{i\omega t} G(t) \\ G(t) &= -i\theta(t) < \{f_{l\sigma}(t), f_{l\sigma}^\dagger\} > \end{aligned} \tag{2.30}$$

where $\{f_{l\sigma}(t), f_{l\sigma}^\dagger\}$ is the anticommutator of the two operators $f_{l\sigma}(t)$ and $f_{l\sigma}^\dagger$,

$$\theta(t) = \begin{cases} 0 & : \quad t < 0 \\ 1 & : \quad t > 0 \end{cases}$$

and $G_{l\sigma}$ is the retarded Green's function and $f(\omega)$ is the Fermi-Dirac distribution function.

To calculate the other two expectation values we will use the same method

$$< f_{l\sigma}^\dagger \psi_{l\sigma} > = \frac{1}{2\pi}\int_{-\infty}^{\infty} d\omega f(\omega) C(\omega)$$

$$\begin{aligned} C(\omega) &= -2Im(F(\omega)) \\ F(\omega) &= \int_{-\infty}^{\infty} dt e^{i\omega t} F(t) \\ F(t) &= -i\theta(t) < \{\psi_{l\sigma}(0,t), f_{l\sigma}^{\dagger}\} > \end{aligned} \tag{2.31}$$

and

$$\begin{aligned} < f_{l+1\sigma}^{\dagger} f_{l\sigma} > &= \frac{1}{2\pi} \int_{-\infty}^{\infty} d\omega f(\omega) B(\omega) \\ B(\omega) &= -2Im(\tilde{G}(\omega)) \\ \tilde{G}(\omega) &= \int_{-\infty}^{\infty} dt e^{i\omega t} \tilde{G}(t) \\ \tilde{G}(t) &= -i\theta(t) < \{f_{l\sigma}(t), f_{l+1\sigma}^{\dagger}\} > \end{aligned} \tag{2.32}$$

Heisenberg equation of motion $i\partial_t A = [A, H]$ is used to calculate the retarded Green's functions and as a result the spectral densities.(From now on, in all our calculations we consider $\hbar = 1$).

$$\begin{aligned} i\partial_t f_{l\sigma}(t) &= [f_{l\sigma}(t), H_{eff}] \\ i\partial_t \psi_{l\sigma}(t) &= [\psi_{l\sigma}(t), H_{eff}] \end{aligned} \tag{2.33}$$

If we substitue $\psi_{l\sigma}$ with equation 2.4 and use equation 2.2 as H_{leads} in H_{eff} equation 2.33 yield

$$\begin{aligned} i\partial_t c_{pl\sigma} &= \varepsilon_p c_{pl\sigma} + \frac{V_0}{\sqrt{V}} f_{l\sigma} \\ i\partial_t f_{l\sigma} &= V_0 \psi_{l\sigma} + \mu_0 f_{l\sigma} + t_0 (f_{l+1\sigma} + f_{l-1\sigma}) \end{aligned} \tag{2.34}$$

By differentiating the retarded Green's functions $G(t), \tilde{G}(t), F(t)$ respect to time we will have

$$\begin{aligned} i\partial_t G(t) &= \delta(t) - i\theta(t) < \{i\partial_t f_{l\sigma}(t), f^\dagger_{l\sigma}\} > \\ i\partial_t \tilde{G}(t) &= -i\theta(t) < \{i\partial_t f_{l\sigma}(t), f^\dagger_{l+1\sigma}\} > \\ i\partial_t F(t) &= -i\theta(t) < \{i\partial_t \psi_{l\sigma}(0,t), f^\dagger_{l\sigma}\} > \end{aligned} \tag{2.35}$$

Inserting equation 2.34 in equation 2.36 and performing the Fourier transform of the results we get the following equations

$$\begin{aligned} \omega G(\omega) &= 1 + V_0 F(\omega) + \mu_0 G(\omega) + 2t_0 \tilde{G}(\omega) \\ \omega \tilde{G}(\omega) &= V_0 \tilde{F}(\omega) + (\mu_0 + t_0)\tilde{G}(\omega) + t_0 G(\omega) \\ \omega F_p(\omega) &= \varepsilon_p F_p(\omega) + \frac{V_0}{\sqrt{V}} G(\omega) \end{aligned} \tag{2.36}$$

where $\tilde{F} = -i\theta(t) < \{\psi_{l\sigma}(0,t), f^\dagger_{l+1\sigma}\} >$ and $F(t) = \frac{1}{\sqrt{V}} \sum_p F_p(t)$ where $F_p(t) = -i\theta(t) < \{c_{pl\sigma}(t), f^\dagger_{l\sigma}\} >$.

Third expression in equation 2.36 can be used to calculate F, as the following

$$\begin{aligned} \omega F_p(\omega) &= \varepsilon_p F_p(\omega) + \frac{V_0}{\sqrt{V}} G(\omega) \\ F_p(\omega) &= \frac{V_0}{\sqrt{V}} \frac{1}{\omega - \varepsilon_p + i\delta} G(\omega) \end{aligned} \tag{2.37}$$

Using $F(\omega) = \frac{1}{\sqrt{V}} \sum_p F_p(\omega)$, we get

$$\begin{aligned} F(\omega) &= V_0 G(\omega) \frac{1}{V} \sum_p \frac{1}{\omega - \varepsilon_p + i\delta} \\ &= V_0 G(\omega) \int_{-\infty}^{\infty} dp \frac{1}{\omega - \varepsilon_p + i\delta} \\ &= V_0 G(\omega) \rho_0 \int_{-\infty}^{\infty} d\varepsilon \frac{1}{\omega - \varepsilon + i\delta} \\ F(\omega) &= -i\pi \rho_0 V_0 G(\omega) \end{aligned} \tag{2.38}$$

whereρ_0 is "density of states" of leads.

Similarly we can calculate $\tilde{F}$ in terms of $\tilde{G}$. It turns out that they have exactly the same relation as F and G: $\tilde{F}(\omega) = -i\pi\rho_0 V_0 \tilde{G}(\omega)$.

we insert $F(\omega) = -i\pi\rho_0 V_0 G(\omega)$ and $\tilde{F}(\omega) = -i\pi\rho_0 V_0 \tilde{G}(\omega)$ in to equation 2.36 and we get the following two-equation two-unknown system

$$\begin{aligned} (\omega - \mu_0 + i\pi\rho_0 V_0^2)G(\omega) - 2t_0\tilde{G}(\omega) &= 1 \\ (\omega - \mu_0 - t_0 + i\pi\rho_0 V_0^2)\tilde{G}(\omega) - t_0 G(\omega) &= 0 \end{aligned} \tag{2.39}$$

Solving for G and $\tilde{G}$ yields

$$\begin{aligned} G(\omega) &= \frac{1}{3}\left(\frac{2}{\omega - \mu_0 + t_0 + i\Gamma} + \frac{1}{\omega - \mu_0 - 2t_0 + i\Gamma}\right) \\ \tilde{G}(\omega) &= \frac{1}{3}\left(\frac{-1}{\omega - \mu_0 + t_0 + i\Gamma} + \frac{1}{\omega - \mu_0 - 2t_0 + i\Gamma}\right) \end{aligned} \tag{2.40}$$

where $\Gamma = \pi\rho_0 V_0^2$. Consequently

$$F(\omega) = \frac{-i\pi\rho_0 V_0}{3}\left(\frac{2}{\omega - \mu_0 + t_0 + i\Gamma} + \frac{1}{\omega - \mu_0 - 2t_0 + i\Gamma}\right) \tag{2.41}$$

Now we have all three retarded Green's function which we need. Using them, we are able to calculate the spectral densities we were to find $A(\omega) = -2ImG(\omega)$, $B(\omega) = -2Im\tilde{G}(\omega)$ and $C(\omega) = -2ImF(\omega)$ and the results are

$$\begin{aligned} A(\omega) &= \frac{2}{3}\left(\frac{2\Gamma}{(\omega - \mu_0 + t_0)^2 + \Gamma^2} + \frac{\Gamma}{(\omega - \mu_0 - 2t_0)^2 + \Gamma^2}\right) \\ B(\omega) &= \frac{2}{3}\left(\frac{-\Gamma}{(\omega - \mu_0 + t_0)^2 + \Gamma^2} + \frac{\Gamma}{(\omega - \mu_0 - 2t_0)^2 + \Gamma^2}\right) \\ C(\omega) &= \frac{-\pi\rho_0 V_0}{3}\left(\frac{2(\omega - \mu_0 + t_0)}{(\omega - \mu_0 + t_0)^2 + \Gamma^2} + \frac{\omega - \mu_0 - 2t_0}{(\omega - \mu_0 - 2t_0)^2 + \Gamma^2}\right) \end{aligned} \tag{2.42}$$

The expectation values in our mean field equations can be calculated using the spectral densities in equation 2.42 and the first equation in equation sets 2.30 2.31 and 2.32. To do so we have to compute integrals of the form

$$\int_{-\infty}^{\infty} d\omega \frac{\Gamma f(\omega)}{(\omega-\varepsilon)^2+\Gamma^2}$$

and

$$\int_{-\infty}^{\infty} d\omega \frac{(\omega-\varepsilon) f(\omega)}{(\omega-\varepsilon)^2+\Gamma^2}$$

. To solve these integrals we apply the following substitution

$$\frac{\Gamma}{(\omega-\varepsilon)^2+\Gamma^2} = \frac{i}{2}\left(\frac{1}{\omega-\varepsilon+i\Gamma} - \frac{1}{\omega-\varepsilon-i\Gamma}\right)$$

and

$$\frac{\omega-\varepsilon}{(\omega-\varepsilon)^2+\Gamma^2} = \frac{1}{2}\left(\frac{1}{\omega-\varepsilon+i\Gamma} + \frac{1}{\omega-\varepsilon-i\Gamma}\right)$$

. By performing the following integrals which the details has been shown in Appendix D, we take a step forward to get final mean field equations

$$\int_{-\infty}^{\infty} d\omega \frac{f(\omega)}{\omega-\varepsilon\pm i\Gamma} = ln\left(\frac{2\pi T}{D}\right) + \Psi\left(\frac{1}{2}+\frac{\Gamma}{2\pi T} \pm \frac{i\varepsilon}{2\pi T}\right) \mp \frac{i\pi}{2} \tag{2.43}$$

where T is the temperature, D is the energy cutoff and Ψ is Digamma function. As a result

$$\begin{aligned}
\int_{-\infty}^{\infty} d\omega \frac{(\omega-\varepsilon) f(\omega)}{(\omega-\varepsilon)^2+\Gamma^2} &= Re\Psi\left(\frac{1}{2}+\frac{\Gamma}{2\pi T}+\frac{i\varepsilon}{2\pi T}\right) + ln\left(\frac{2\pi T}{D}\right) \\
\int_{-\infty}^{\infty} d\omega \frac{\Gamma f(\omega)}{(\omega-\varepsilon)^2+\Gamma^2} &= -Im\Psi\left(\frac{1}{2}+\frac{\Gamma}{2\pi T}+\frac{i\varepsilon}{2\pi T}\right) + \frac{\pi}{2}
\end{aligned} \tag{2.44}$$

In the limit $T \to 0$ which we are finally interested in, $\frac{\Gamma \pm i\varepsilon}{2\pi T} \gg \frac{1}{2}$ so $\Psi(\frac{1}{2}+\frac{\Gamma}{2\pi T} \pm \frac{i\varepsilon}{2\pi T}) \approx \Psi(\frac{\Gamma}{2\pi T} \pm \frac{i\varepsilon}{2\pi T})$. Using $\Psi(z) \approx ln(z)$, for $|z| \gg 1$, we will have

$$\Psi\left(\frac{\Gamma}{2\pi T} \pm \frac{i\varepsilon}{2\pi T}\right) \approx ln\left(\frac{\sqrt{\Gamma^2+\varepsilon^2}}{2\pi T}\right) \pm iArctan\frac{\varepsilon}{\Gamma} \tag{2.45}$$

By substituting equation 2.45 for Ψ in equation 2.44 we obtain zero temperature limit expressions

$$\begin{aligned}\int_{-\infty}^{\infty} d\omega \frac{(\omega-\varepsilon)f(\omega)}{(\omega-\varepsilon)^2+\Gamma^2} &\approx ln(\frac{\sqrt{\Gamma^2+\varepsilon^2}}{D}) \\ \int_{-\infty}^{\infty} d\omega \frac{\Gamma f(\omega)}{(\omega-\varepsilon)^2+\Gamma^2} &\approx \frac{\pi}{2} - 2Arctan\frac{\varepsilon}{\Gamma}\end{aligned} \tag{2.46}$$

Using equation 2.46 to perform $\frac{1}{2\pi}\int_{-\infty}^{\infty} d\omega f(\omega)X(\omega)$, where $X(\omega)$ can be $A(\omega)$ or $B(\omega)$ or $C(\omega)$ in equation 2.42,results in the following as our mean field equations

$$\begin{aligned} n &= \frac{1}{2} - \frac{2}{3\pi}Arctan\frac{\gamma_1}{\Gamma} - \frac{1}{3\pi}Arctan\frac{\gamma_2}{\Gamma} \\ \eta &= \frac{1}{3\pi}Arctan\frac{\gamma_1}{\Gamma} - \frac{1}{3\pi}Arctan\frac{\gamma_2}{\Gamma} \\ \chi &= \frac{-\rho_0 V_0}{6}(2ln(\frac{\sqrt{\Gamma^2+\gamma_1^2}}{D}) + ln(\frac{\sqrt{\Gamma^2+\gamma_2^2}}{D})) \end{aligned} \tag{2.47}$$

where $\gamma_1 = \mu_0 - t_0$ and $\gamma_2 = \mu_0 + 2t_0$. If we simplify the last equation of 2.47 and insert the identity $\chi = \frac{-V_0}{J_K + \frac{2J'_K}{3}}$ the following equation can be obtained

$$\frac{\rho_0}{6}(2ln(\frac{\sqrt{\Gamma^2+\gamma_1^2}}{T_K} + ln(\frac{\sqrt{\Gamma^2+\gamma_2^2}}{T_K})) = 0 \tag{2.48}$$

where T_K is the Kondo temperature of our system and it has been defined in the following

$$T_K = Dexp\left[\frac{1}{\frac{-\rho_0}{2}(J_K + \frac{2J'_K}{3})}\right] \tag{2.49}$$

Equations in 2.47 has to be solved self-consistently which is the subject of the next section.

2.3 Mean-Field Equations: Self-Consistent Solutions

In order to probe the case of quantum phase transition, in this section, we need to solve the equations we have obtained in previous sections. By combining equations 2.47, 2.48 and 2.29, and after some simple algebra we get the following equations

$$\begin{aligned}
0 &= n - 0.5 + 0.21 Arctan \frac{J(\frac{4\alpha+1}{12} - 0.042n + 1.17\eta)}{\Gamma} \\
&\quad + 0.11 Arctan \frac{J(-\frac{4\alpha+1}{6} + 0.083n - 2.08\eta)}{\Gamma} \\
0 &= \eta - 0.11 Arctan \frac{J(\frac{4\alpha+1}{12} - 0.042n + 1.17\eta)}{\Gamma} \\
&\quad + 0.11 Arctan \frac{J(-\frac{4\alpha+1}{6} + 0.083n - 2.08\eta)}{\Gamma} \\
0 &= \left[J^2 (\frac{4\alpha+1}{12} - 0.042n + 1.17\eta)^2 + \Gamma^2 \right] \\
&\quad \times \sqrt{J^2 (-\frac{4\alpha+1}{6} + 0.083n - 2.08\eta)^2 + \Gamma^2} - 1
\end{aligned} \tag{2.50}$$

where α is t/J and $J' = J/4$. All the quantities with dimension of energy have been measured in the units of T_K.

The code presented in Appendix F, has been used to solve this system of equations. The details of calculations are also presented in Appendix F. But physically acceptable results have not been obtained. Here we present sample result from reference [33]. The following graphs are results we expected to get in certain regimes of parameters

As we can see in figures 2.4,2.5 and 2.6, by tuning J we have a case of quantum phase transition. As J increases, the ratio of J/J_K will also increase. As a result system undergoes a phase transition from Kondo regime to non-Kondo regime where $\Gamma = 0$ because $\chi = 0$. We also can see in the pictures that for different values of t, Γ goes to zero discontinuously, this means the first derivative of free energy (χ) is discontinuous and as a result we are dealing with a case of "first order quantum phase

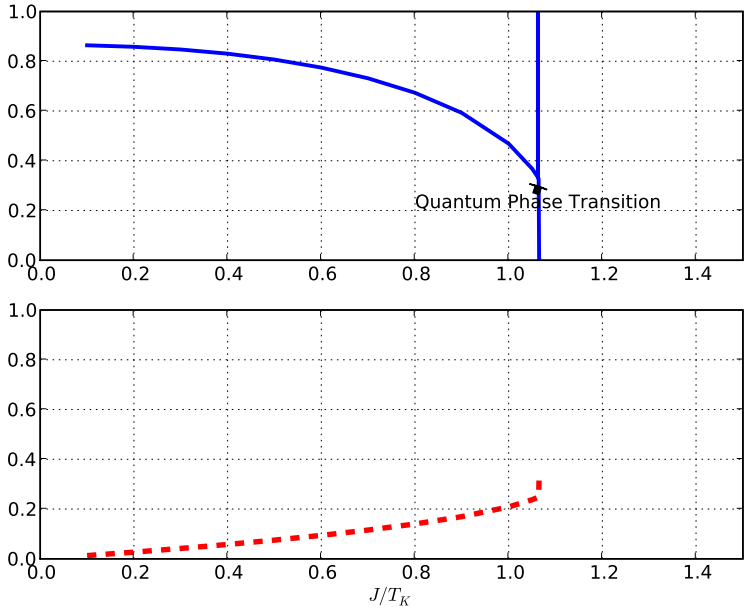

Figure 2.4: Blue Graph Represent $\Gamma = \pi\rho_0 V_0^2$ where V_0 depends on mean-field variable χ. The dashed red line represents mean-field variable η. By tuning J a quantum phase transition will happen.($t = 4J$) By tuning the coupling constants, a competition will happen between two states. One is the state of singlet between the electron on the dot and the virtual bound state in the lead. The other is formation of singlet between two neighbour dots. At the poit of phase transition which we can see in the graph, the second phase (neighbour dot singlet) gets dominant knowing that before that particular point (particular value of J) the first phase ("Kondo singlet") was dominant.By tuning the coupling constants, a competition will happen between two states. One is the state of singlet between the electron on the dot and the virtual bound state in the lead. The other is formation of singlet between two neighbour dots. At the poit of phase transition which we can see in the graph, the second phase (neighbour dot singlet) gets dominant knowing that before that particular point (particular value of J) the first phase ("Kondo singlet") was dominant.

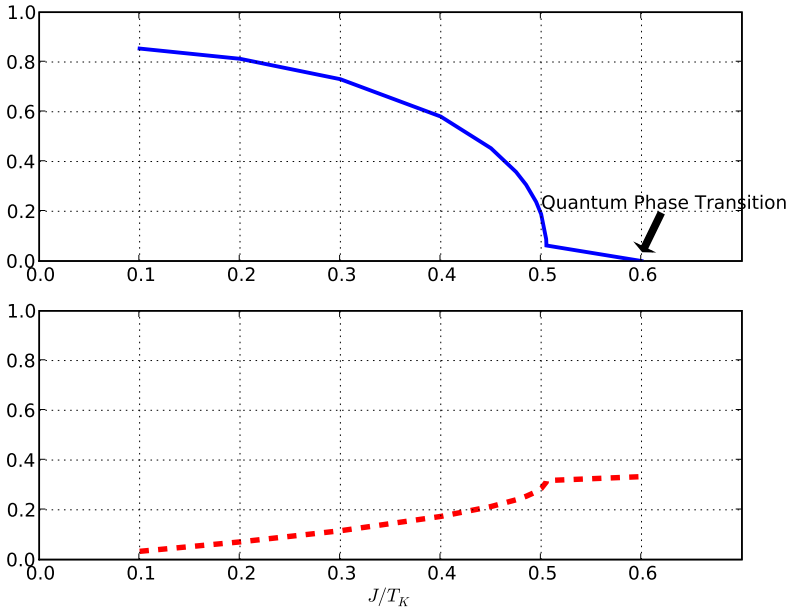

Figure 2.5: Blue Graph Represent $\Gamma = \pi\rho_0 V_0^2$ where V_0 depends on mean-field variable χ. The dashed red line represents mean-field variable η. By tuning J a quantum phase transition will happen.$t = 10J$

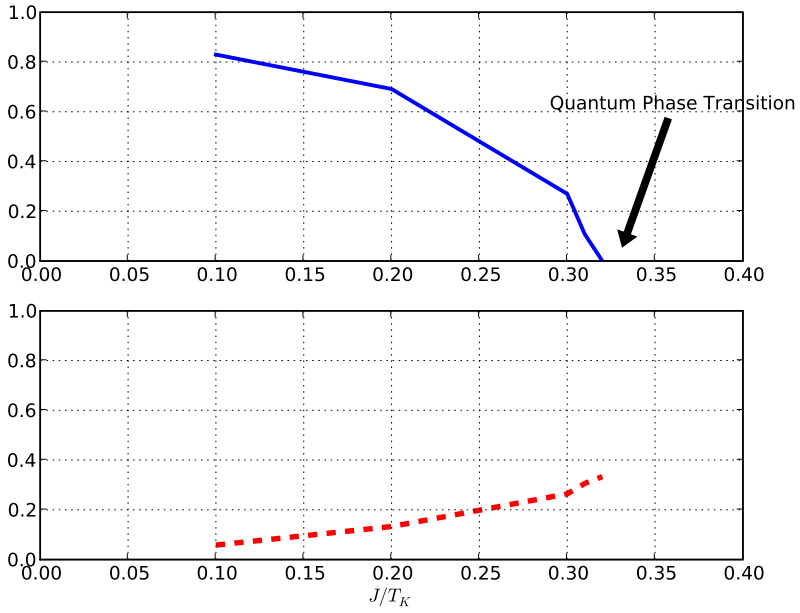

Figure 2.6: Blue Graph Represent $\Gamma = \pi\rho_0 V_0^2$ where V_0 depends on mean-field variable χ. The dashed red line represents mean-field variable η. By tuning J a quantum phase transition will happen.$t = 17J$

transition". But we have to notice that as t increases the first order characteristic of the phase transition becomes weaker. This is apparent if we consider how fast $\Gamma \rightarrow 0$ (meaning the derivative of it which is practically infinite for the case of $t/J = 4$)when the ratio of t/J increases. In the next chapter we see the consequences of this phenomenon on transport.

Chapter 3

Calculation of Transport

Our main result in the last chapter was the effective Hamiltonian of triple-dot system. In this chapter, we are going to calculate conductance and current-fluctuations of the quantum dot system, using the effective Hamiltonian. Our main goal here is to probe quantum phase transition impacts on the transport.

3.1 Scattering Formalism and Triple-Dot Scattering Matrix

Due to a scatterer potential in one dimension, a beam of incoming particles splits in two, the reflected beam and the transmitted beam. Dependent on the scatterer potential characteristics, reflection and transmission coefficients can be calculated using boundary conditions for different regions.

Figure 3.1: Schematic figure of 1 dimensional scattering

In this case as we can see in figure 3.1 the wave function in different regions is

$$\psi(x) = \begin{cases} Ae^{ikx} + Be^{-ikx} & : \quad regionI \\ Cf(x) + Dg(x) & : \quad regionII \\ Fe^{ikx} + Ge^{-ikx} & : \quad regionIII \end{cases}$$

Coefficients of the wave function(A, B, F, G) in the regions I and III are related by the scattering matrix which depends on the properties of the scatterer potential in region II. To investigate the transport properties, only these coefficients and consequently the scattering matrix are important. In our problem the regionII is our triple-dot system. We are going to calculate the transport properties through these dots.

As the first step we need to specify our leads properties. In comparison with the 1D scattering theory, our leads play the role of regions I and III. As a result leads and states of their electrons play an important part in stating the details of transport calculation. We consider electrons in leads as plane waves. After arriving to the scattering center, the beam of electrons will split in a reflected beam which goes back to the same lead and a transmitted beam which propagates in other two leads. According to these consideration, creation and annihilation of electrons in different leads can be described by a second quantized operator ψ

$$\psi_{l\sigma}(x,t) = \begin{cases} \frac{1}{\sqrt{V}} \sum_p e^{ipx - i\varepsilon_p t} A_{pl\sigma} & : \quad x < 0 \\ \frac{1}{\sqrt{V}} \sum_p e^{ipx - i\varepsilon_p t} B_{pl\sigma} & : \quad x > 0 \end{cases}$$

According to the $\psi_{l\sigma}$ expression, we have considered a one dimensional lead which its electrons get scattered by triple-dot system. $A_{pl\sigma}$ and $B_{pl\sigma}$ are annihilation operators and they describe incoming and outgoing wave/particles($\frac{e^{ipx}}{\sqrt{V}}$ is a simplified scattering state). These operators do not have any difference from c_{lps} in equation 2.2. We have chosen different names to distinguish the incoming and outgoing electrons. As a matter of fact, this distinction will be helpful to calculate the transport. We also need to write the Hamiltonian of leads in a way that reflects the properties we

are going to use to calculate transport, including $\psi_{l\sigma}$ and consequently A and B. To fulfill this purpose we use one dimensional Dirac Hamiltonian

$$H_{leads} = -iv_F \sum_l \int_{-L}^{L} dx \psi_l^\dagger \partial_x \psi_l \tag{3.1}$$

(v_F is Fermi velocity) this Hamiltonian for leads is equivalent to the Hamiltonian we have used to describe leads in previous section.

The origin of our one dimensional coordinate is at triple-dot system ($x = 0$). So the $x > 0$ part of $\psi_{l\sigma}$ shows that the electron has left the lead. While $x < 0$ is associated with reflected electrons. $\psi_{l\sigma}$ is a second quantized operator which annihilates an electron in the l_{th} lead with spin σ. Consequently, $\psi_{l\sigma}^\dagger$ creates a an electron in the l_{th} lead with spin σ.

Since the observables and their expectation values which we are interested in, will be expressed in terms of creation and annihilation operator products, we need to specify their expectation values. Using $A_{pl\sigma}$, the distribution function of the incoming particles will be

$$< A_{pl\sigma}^\dagger A_{p'l'\sigma'} >= \delta_{pp'}\delta_{ll'}\delta_{\sigma\sigma'} f_l(\varepsilon_p) \tag{3.2}$$

where $f_l(\varepsilon_p) = f(\varepsilon_p - \mu_l)$ and f is Fermi-Dirac distribution function and μ_l is the chemical potential of l_{th} lead.

As mentioned earlier, to calculate the transport properties, we need to find the scattering matrix of our system. To do so, we have to find $B_{pl\sigma}$ in terms of $A_{pl\sigma}$ by applying the boundary conditions. These conditions will be applied when we use the Heisenberg equation of motion $i\partial_t X = [X, H]$ for operators of our system. The role of scattering center comes up in this part of the calculation. We use the effective Hamiltonian, obtained in the previous chapter, in the Heisenberg equation of motion. H_{eff} includes the property of the scattering center.

$$\begin{aligned} H_{eff} &= t_0 \sum_l (f^\dagger_{l+1s} f_{ls} + f^\dagger_{ls} f_{l+1s}) \\ &+\mu_0 \sum_l f^\dagger_{ls} f_{ls} + V_0 \sum_l (\psi^\dagger_{ls}(0) f_{ls} + f^\dagger_{ls} \psi_{ls}(0)) \\ &+H_{leads} \end{aligned} \tag{3.3}$$

where H_leads is one dimensional Dirac Hamiltonian.

Now we have all the ingredients to perform our calculations. Using the Heisenberg equation of motion for the $\psi_{l\sigma}(t)$ and $f_{l\sigma}(t)$ we get the following results

$$\begin{aligned} (\mu_0 - \varepsilon_p) f_{pl\sigma} + \frac{V_0}{2}(A_{pl\sigma} + B_{pl\sigma}) + t_0(f_{pl+1\sigma} + f_{pl-1\sigma}) &= 0 \\ iv_F(B_{pl\sigma} - A_{pl\sigma}) - V_0 f_{pl\sigma} &= 0 \end{aligned} \tag{3.4}$$

In equation 3.4 $f_{pl\sigma}$ comes from the mode expansion of $f_{l\sigma}(t) = \frac{1}{\sqrt{V}} \sum_p e^{-i\varepsilon_p t} f_{pl\sigma}$. Because $\psi_{l\sigma}$ is not continuous at $x = 0$ we use the following expressions for its value at $x = 0$

$$\psi_{l\sigma}(0) = \frac{1}{2}(\psi_{l\sigma}(\epsilon) + \psi_{l\sigma}(-\epsilon)) \tag{3.5}$$

where $\epsilon > 0$ and $\epsilon \to 0$

After some algebra which includes shifting indices to get proper relations for $l-1$ and $l+1$ case, we can eliminate $f_{pl\sigma}$ form equation 3.4 and get the following relation between $A_{pl\sigma}, A_{pl\pm1\sigma}$ and $B_{pl\sigma}$

$$B_{pl\sigma} = rA_{pl\sigma} + t(A_{pl-1\sigma} + A_{pl+1\sigma}) \tag{3.6}$$

where r and t are

$$r = \frac{\beta\alpha + \frac{2t_0}{V_0}\beta - 2(\frac{2t_0}{V_0})^2}{\alpha^2 + \frac{2t_0}{V_0}\alpha - 2(\frac{2t_0}{V_0})^2}$$

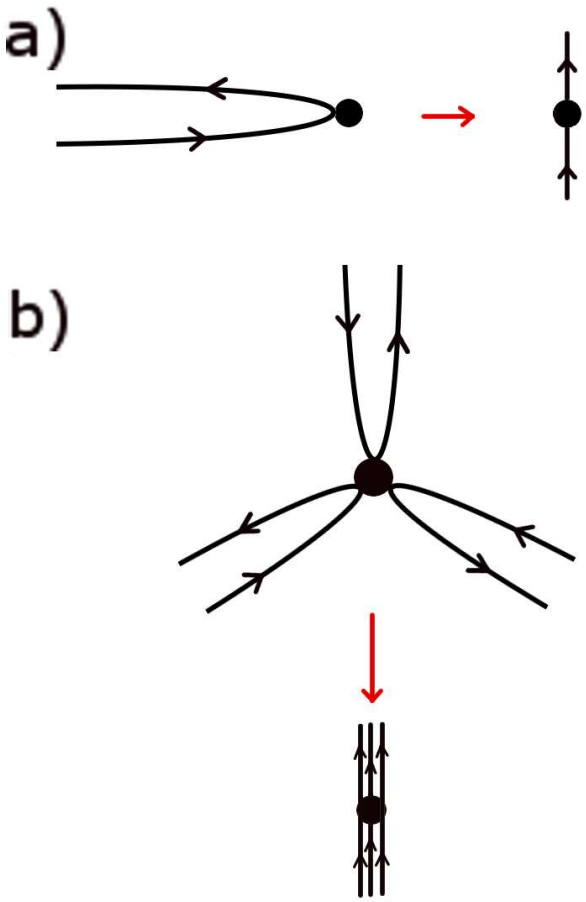

Figure 3.2: (a) representation of one lead. (b) representation of our system with the (a) substitution. Big black circle represent the triple-dot system which is also the scatterer. The spatial extention of the leads of our system in this picture is from $-\infty$ to $+\infty$, but the extention of the leads are actually form $-\infty$ to the dot. The extended part represents the section which reflected particles enter. The structure of the triple dot does not appear in this picture, but in calculations this structure will be taken into account.

$$t = \frac{\frac{-4it_0}{v_F}}{\alpha^2 + \frac{2t_0}{V_0}\alpha - 2(\frac{2t_0}{V_0})^2} \tag{3.7}$$

where α and β are

$$\begin{aligned} \alpha &= \frac{2(\mu_0 - \varepsilon_p)}{V_0} - \frac{iV_0}{v_F} \\ \beta &= \frac{2(\mu_0 - \varepsilon_p)}{V_0} + \frac{iV_0}{v_F} \end{aligned} \tag{3.8}$$

r and t are elements of scattering matrix

$$S = \begin{pmatrix} r & t & t \\ t & r & t \\ t & t & r \end{pmatrix}$$

Since the scattering matrix is unitary $S^\dagger S = I$ we have the following relations between r and t (we consider $tt^* = T$ and $rr^* = R$)

$$\begin{aligned} R + 2T &= 1 \\ T + rt^* + tr^* &= 0 \end{aligned} \tag{3.9}$$

3.2 Conductance and Current-Current Correlation Function

3.2.1 Conductance

Now that we have the scattering matrix, we can now calculate the transport. We can define the current operator [35] as

$$\hat{I}_l(t) = e \sum_{ps} \sum_{p's'} (A^\dagger_{lps} A_{lp's'} - B^\dagger_{lps} B_{lp's'}) e^{i(\varepsilon_{p'} - \varepsilon_p)t} \tag{3.10}$$

The above definition has been derived in details in [35] starting by the probability current. The above formula simply counts the number of reflected electrons and the number of transmitted electrons from the l_{th} lead (According to the [35][36] this formula is valid only for small frequencies). We are interested in calculating the current in frequency space so we take the Fourier transform of 3.10

$$\hat{I}_l(\omega) = e\sum_{ps}\sum_{p's'}(A^{\dagger}_{lps}A_{lp's'} - B^{\dagger}_{lps}B_{lp's'})2\pi\delta(\varepsilon_{p'} - \varepsilon_p - \omega) \tag{3.11}$$

Consequently the expectation value of the current in the l_{th} lead will be

$$\begin{aligned} < \hat{I}_l(\omega) > &= e\sum_{ps}\sum_{p's'}(< A^{\dagger}_{lps}A_{lp's'} > - < B^{\dagger}_{lps}B_{lp's'} >)2\pi\delta(\varepsilon_{p'} - \varepsilon_p - \omega) \\ &= 2\pi e\sum_{ps}\sum_{p's'}\delta_{pp'}\delta_{ss'}\left[f_l(\varepsilon_p) - Rf_l(\varepsilon_p) - Tf_{l-1}(\varepsilon_p) - Tf_{l+1}(\varepsilon_p)\right] \\ &\quad \times\delta(\varepsilon_{p'} - \varepsilon_p - \omega) \\ &= 4\pi e\sum_{p} T\left[2f_l(\varepsilon_p) - f_{l-1}(\varepsilon_p) - f_{l+1}(\varepsilon_p)\right]\delta(\omega) \end{aligned} \tag{3.12}$$

We have used equations 3.9, 3.6 and 3.2. We consider linear response regime $f_l(\varepsilon_p) = f(\varepsilon_p - \mu_l) = f(\varepsilon_p) - \mu_l\frac{\partial f}{\partial\varepsilon_p}$ and we also use $2\pi\sum_p \to \rho_0\int d\varepsilon$. so we end up at

$$< \hat{I}_l(\omega) >= 2e\delta(\omega)\rho_0(\mu_{l+1} + \mu_{l-1} - 2\mu_l)\int_{-\infty}^{\infty} d\varepsilon T(\varepsilon)\frac{\partial f}{\partial\varepsilon} \tag{3.13}$$

As mentioned previously, we are interested in zero temperature limit and $\frac{\partial f}{\partial\varepsilon} = -\delta(\varepsilon)$ in this limit. As a result

$$< \hat{I}_l(\omega) >= 2e\delta(\omega)\rho_0(\mu_{l+1} + \mu_{l-1} - 2\mu_l)T(\varepsilon = 0) \tag{3.14}$$

where $T(\varepsilon = 0) = tt^*|_{\varepsilon=0}$ and based on equations 3.7 and 3.8 we have the following relation for T

$$T = \frac{8}{9}\frac{V_0^2}{v_F^2}Re\left[\frac{a}{\alpha - \frac{2t_0}{V_0}} + \frac{b}{\alpha + \frac{4t_0}{V_0}}\right] \tag{3.15}$$

where

$$\begin{aligned} a &= \frac{-iv_F}{2V_0} - \frac{1}{2\left[\frac{3t_0}{V_0} + \frac{iV_0}{v_F}\right]} \\ b &= \frac{-iv_F}{2V_0} + \frac{1}{2\left[\frac{3t_0}{V_0} - \frac{iV_0}{v_F}\right]} \end{aligned} \tag{3.16}$$

this expression for T makes upcoming integrals performance easier. We consider $\gamma_1 = \mu_0 - t_0$ and $\gamma_2 = \mu_0 + 2t_0$ same as previous chapter and we also define $\Gamma_0 = \frac{V_0^2}{2v_F}$. The ε dependence of T is in α (3.8). If we insert a and b, after some algebra we gain

$$\begin{aligned} T(\varepsilon) &= \frac{\frac{2t_0V_0^2}{3v_F^2}}{(\frac{3t_0}{V_0})^2 + (\frac{V_0}{v_F})^2} \frac{\varepsilon - \gamma_1}{(\varepsilon-\gamma_1)^2 + \Gamma_0^2} \\ &\quad - \frac{\frac{2t_0V_0^2}{3v_F^2}}{(\frac{3t_0}{V_0})^2 + (\frac{V_0}{v_F})^2} \frac{\varepsilon - \gamma_2}{(\varepsilon-\gamma_2)^2 + \Gamma_0^2} \\ &\quad + \frac{\frac{(t_0V_0)^2}{3v_F^2}}{(\frac{3t_0}{V_0})^2 + (\frac{V_0}{v_F})^2} \frac{1}{(\varepsilon-\gamma_1)^2 + \Gamma_0^2} \\ &\quad + \frac{\frac{(t_0V_0)^2}{3v_F^2}}{(\frac{3t_0}{V_0})^2 + (\frac{V_0}{v_F})^2} \frac{1}{(\varepsilon-\gamma_2)^2 + \Gamma_0^2} \end{aligned} \tag{3.17}$$

and to calculate the expectation value of current operator (equation 3.14) we have to substitute $\varepsilon = 0$. As the next step we have to determine the chemical potentials of the leads. We consider two cases. First case: one lead as source and two others as drains and Second case: two sources and one drain. Because we are in linear response regime these chemical potentials are very close to the Fermi energy. We choose $\pm V/3$ as voltage of source (+) and drain (-).

Case One: One Source and Two Drains

In this case we consider the l_{th} lead is the source. Consequently, according to equation 3.14, we have

$\mu_l = V/3$; $\mu_{l+1} = \mu_{l-1} = -V/3$

$I_l \propto -4V/3$

$I_{l+1}, I_{l-1} \propto 2V/3$

as a result the conductance, $G_l = \partial I_l/\partial V$, if we measure respect to different leads will be:

$$\begin{aligned} G_l &= \frac{-8e\rho_0 T(\varepsilon=0)}{3} \\ G_{l+1} = G_{l-1} &= \frac{4e\rho_0 T(\varepsilon=0)}{3} \end{aligned} \tag{3.18}$$

Case2: Two Source and One Drain:

$\mu_l = \mu_{l+1} = V/3$; $\mu_{l-1} = -V/3$

$I_l, I_{l+1} \propto -2V/3$

$I_{l-1} \propto 4V/3$

consequently

$$\begin{aligned} G_l = G_{l+1} &= \frac{-4e\rho_0 T(\varepsilon=0)}{3} \\ G_{l-1} &= \frac{8e\rho_0 T(\varepsilon=0)}{3} \end{aligned} \tag{3.19}$$

Now if we use the result of chapter 2, and use the values of mean-field variables we will obtain the following graphs for conductance of the drains only. Blue lines show conductance in case one and red lines represent the second case. We plot $G/e\rho_0$.

Conductance of our system and Γ in different parameter regimes behave similarly.(T does not depend on the derivative of mean-field variables, as a consequence this behaviour is reasonable.)

3.2.2 Current-Current Correlation Function

In our attempt of investigating transport, we are going to calculate current-current fluctuations in this section. Current-current fluctuations $S_{\alpha\beta}$ is determined by the

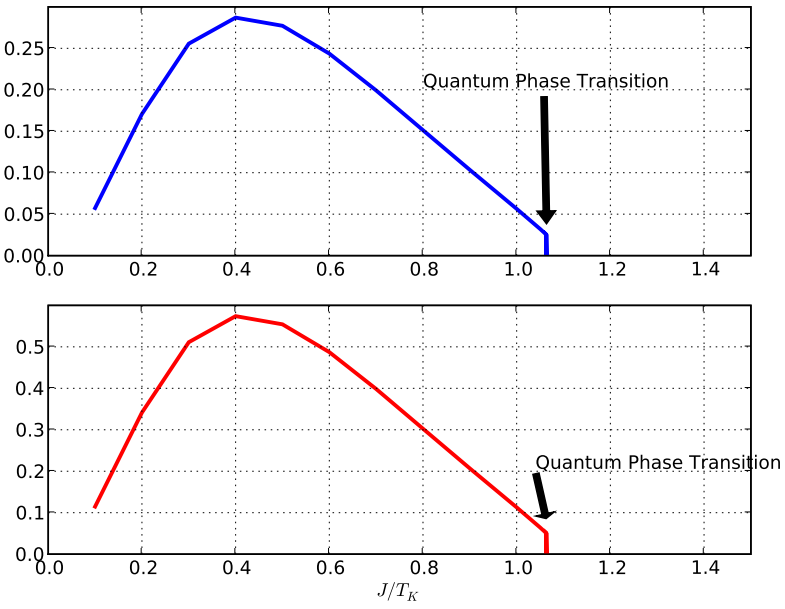

Figure 3.3: Conductance of Drains,$t = 4J$

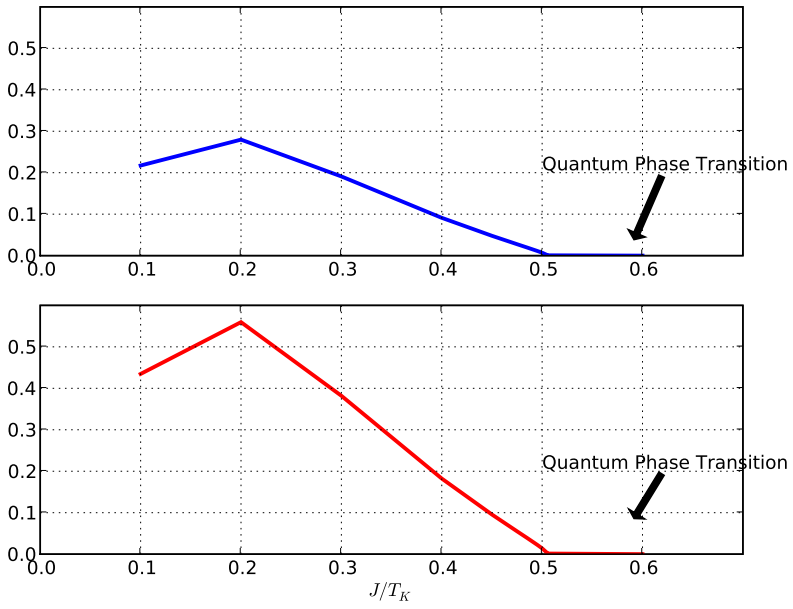

Figure 3.4: Conductance of Drains,$t = 10J$

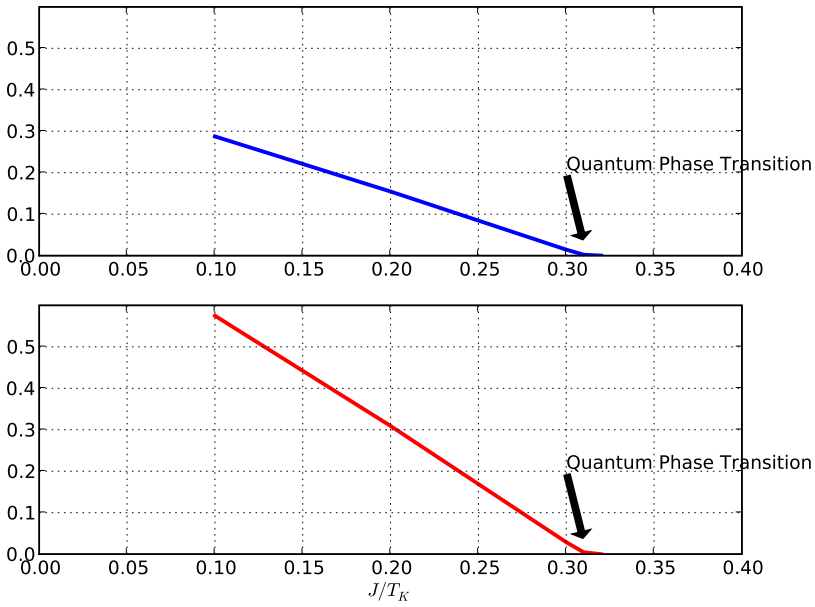

Figure 3.5: Conductance of Drains,$t = 17J$

expectation value of the Fourier transformed current operator $\hat{I}_\alpha(\omega)$ through the relation [35]

$$\frac{1}{2} < \Delta\hat{I}_\alpha(\omega)\Delta\hat{I}_\beta(\omega') + \Delta\hat{I}_\beta(\omega')\Delta\hat{I}_\alpha(\omega) > \equiv 2\pi S_{\alpha\beta}(\omega)\delta(\omega+\omega') \tag{3.20}$$

where α and β represent different leads, and

$$\Delta\hat{I}_\alpha(\omega) = \hat{I}_\alpha(\omega) - < \hat{I}_\alpha(\omega) > \tag{3.21}$$

Inserting 3.21 in the frist term of left hand side of equation 3.20 results in

$$< \Delta\hat{I}_\alpha(\omega)\Delta\hat{I}_\beta(\omega') > = < \hat{I}_\alpha(\omega)\hat{I}_\beta(\omega') > - < \hat{I}_\alpha(\omega) >< \hat{I}_\beta(\omega') > \tag{3.22}$$

where $\hat{I}$ is the same as equation 3.12. If we use the current expression in equation 3.22 we get

$$\begin{aligned}\hat{I}_l(\omega)\hat{I}_{l'}(\omega') = (2\pi e)^2 \sum_{ps}\sum_{p's'}\sum_{p''s''}\sum_{p'''s'''} \quad & \delta(\varepsilon_{p'} - \varepsilon_p + \omega)\delta(\varepsilon_{p'''} - \varepsilon_{p''} + \omega') \\ & \times \left[A^\dagger_{lps}A_{lp's'} - B^\dagger_{lps}B_{lp's'}\right] \\ & \times \left[A^\dagger_{l'p''s''}A_{l'p'''s'''} - B^\dagger_{l^{prime}p''s''}B_{l'p'''s'''}\right]\end{aligned} \tag{3.23}$$

As the next step, we do the multiplication and then we insert the equation 3.6 in the formula instead of each B(for $B^\dagger$ we simply use the complex conjugate of B). We need to calculate the expectation value of 3.23 in order to get S. If we do so, terms like $< A^\dagger_{lps}A_{l'p's'}A^\dagger_{l''p''s''}A_{l'''p'''s'''} >$ come up.

To deal with these terms, we use the Wick's theorem. The main idea of this theorem is that the expectation value is non-zero only if it contains two pairs of operators with the same indices. So we get a contribution from normal pairing i.e.,$l = l'$, $p = p'$, $s = s'$, and $l'' = l'''$, $p'' = p'''$, $s'' = s'''$ and also exchange pairing,$l = l'''$,

$p = p'''$, $s = s'''$, and $l' = l''$, $p' = p''$, $s' = s''$. The following identity is the final expectation value

$$\begin{aligned} < A^{\dagger}_{lps} A_{l'p's'} A^{\dagger}_{l''p''s''} A_{l'''p'''s'''} > &= \delta_{ll'}\delta_{pp'}\delta_{ss'}\delta_{l''l'''}\delta_{p''p'''}\delta_{s''s'''} f_l(\varepsilon_p) f_{l''}(\varepsilon_{p''}) \\ &+ \delta_{ll'''}\delta_{pp'''}\delta_{ss'''}\delta_{l'l''}\delta_{p'p''}\delta_{s's''} f_l(\varepsilon_p)(1 - f_{l'}(\varepsilon_{p'})) \end{aligned} \tag{3.24}$$

first term represents the normal pairing and second term represents exchange pairing. If we look more precise, we understand that the first term (normal pairing) is $< A^{\dagger}_{lps} A_{l'p's'} >< A^{\dagger}_{l''p''s''} A_{l'''p'''s'''} >$. After inserting 3.24, these normal pairing produce $< \hat{I}_\alpha >< \hat{I}_\beta >$. Consequently $\Delta\hat{I}_\alpha \Delta\hat{I}_\beta$(equation 3.22) contains only the exchange pairings.

Since our system possesses only three leads and since equation 3.20 is insensitive to switching indices, we only need to calculate S_{ll} and S_{ll-1}. After simple but long algebra we get the following equations for S_{ll}(intralead correlation) and S_{ll-1}(interlead correlation)

Intralead correlation:

$$\begin{aligned} integrand1 = &(1 - R(\varepsilon))(1 - R(\varepsilon + \omega)) \left[f_l(\varepsilon)(1 - f_l(\varepsilon + \omega)) + f_l(\varepsilon + \omega)(1 - f_l(\varepsilon)) \right] \\ &+ R(\varepsilon) T(\varepsilon + \omega) \left[f_l(\epsilon)(1 - f_{l-1}(\varepsilon + \omega)) + f_{l-1}(\varepsilon + \omega)(1 - f_l(\varepsilon)) \right] \\ &+ R(\varepsilon) T(\varepsilon + \omega) \left[f_l(\varepsilon)(1 - f_{l+1}(\varepsilon + \omega)) + f_{l+1}(\varepsilon + \omega)(1 - f_l(\varepsilon)) \right] \\ &+ R(\varepsilon + \omega) T(\varepsilon) \left[f_{l-1}(\varepsilon)(1 - f_l(\varepsilon + \omega)) + f_l(\varepsilon + \omega)(1 - f_{l-1}(\varepsilon)) \right] \\ &+ R(\varepsilon + \omega) T(\varepsilon) \left[f_{l+1}(\varepsilon)(1 - f_l(\varepsilon + \omega)) + f_l(\varepsilon + \omega)(1 - f_{l+1}(\varepsilon)) \right] \\ &+ T(\varepsilon + \omega) T(\varepsilon) \left[f_{l-1}(\varepsilon)(1 - f_{l-1}(\varepsilon + \omega)) + f_{l-1}(\varepsilon + \omega)(1 - f_{l-1}(\varepsilon)) \right] \\ &+ T(\varepsilon + \omega) T(\varepsilon) \left[f_{l+1}(\varepsilon)(1 - f_{l+1}(\varepsilon + \omega)) + f_{l+1}(\varepsilon + \omega)(1 - f_{l+1}(\varepsilon)) \right] \\ &+ T(\varepsilon + \omega) T(\varepsilon) \left[f_{l-1}(\varepsilon)(1 - f_{l+1}(\varepsilon + \omega)) + f_{l+1}(\varepsilon + \omega)(1 - f_{l-1}(\varepsilon)) \right] \end{aligned}$$

$$+T(\varepsilon+\omega)T(\varepsilon)\left[f_{l+1}(\varepsilon)(1-f_{l-1}(\varepsilon+\omega))+f_{l-1}(\varepsilon+\omega)(1-f_{l+1}(\varepsilon))\right] \quad (3.25)$$

$$S_{ll}=2e^2\rho_0^2\delta(\omega+\omega')\int_{-\infty}^{\infty}\mathrm{d}\varepsilon(integrand1) \quad (3.26)$$

Interlead Correlation:

$$\begin{aligned}
integrand2 = {} & r(\varepsilon)r^*(\varepsilon+\omega)t^*(\varepsilon)t(\varepsilon+\omega)\left[f_l(\varepsilon)(1-f_l(\varepsilon+\omega))+f_l(\varepsilon+\omega)(1-f_l(\varepsilon))\right] \\
& -t^*(\varepsilon)t(\varepsilon+\omega)\left[f_l(\varepsilon)(1-f_l(\varepsilon+\omega))+f_l(\varepsilon+\omega)(1-f_l(\varepsilon))\right] \\
& +r^*(\varepsilon)r(\varepsilon+\omega)t(\varepsilon)t^*(\varepsilon+\omega)\left[f_{l-1}(\varepsilon)(1-f_{l-1}(\varepsilon+\omega))+f_{l-1}(\varepsilon+\omega)(1-f_{l-1}(\varepsilon))\right] \\
& -t(\varepsilon)t^*(\varepsilon+\omega)\left[f_{l-1}(\varepsilon)(1-f_{l-1}(\varepsilon+\omega))+f_{l-1}(\varepsilon+\omega)(1-f_{l-1}(\varepsilon))\right] \\
& +t^*(\varepsilon)t^*(\varepsilon+\omega)r(\varepsilon)r(\varepsilon+\omega)\left[f_l(\epsilon)(1-f_{l-1}(\varepsilon+\omega))+f_{l-1}(\varepsilon+\omega)(1-f_l(\varepsilon))\right] \\
& +t(\varepsilon)t(\varepsilon+\omega)r^*(\varepsilon)r^*(\varepsilon+\omega)\left[f_{l-1}(\varepsilon)(1-f_l(\varepsilon+\omega))+f_l(\varepsilon+\omega)(1-f_{l-1}(\varepsilon))\right] \\
& +r(\varepsilon)t^*(\varepsilon)T(\varepsilon+\omega)\left[f_l(\varepsilon)(1-f_{l+1}(\varepsilon+\omega))+f_{l+1}(\varepsilon+\omega)(1-f_l(\varepsilon))\right] \\
& +r^*(\varepsilon+\omega)t(\varepsilon+\omega)T(\varepsilon)\left[f_{l+1}(\varepsilon)(1-f_l(\varepsilon+\omega))+f_l(\varepsilon+\omega)(1-f_{l+1}(\varepsilon))\right] \\
& +T(\varepsilon+\omega)r^*(\varepsilon)t(\varepsilon)\left[f_{l-1}(\varepsilon)(1-f_{l+1}(\varepsilon+\omega))+f_{l+1}(\varepsilon+\omega)(1-f_{l-1}(\varepsilon))\right] \\
& +t^*(\varepsilon+\omega)r(\varepsilon+\omega)T(\varepsilon)\left[f_{l+1}(\varepsilon)(1-f_{l-1}(\varepsilon+\omega))+f_{l-1}(\varepsilon+\omega)(1-f_{l+1}(\varepsilon))\right] \\
& +T(\varepsilon+\omega)T(\varepsilon)\left[f_{l+1}(\varepsilon)(1-f_{l+1}(\varepsilon+\omega))+f_{l+1}(\varepsilon+\omega)(1-f_{l+1}(\varepsilon))\right] \quad (3.27)
\end{aligned}$$

$$S_{ll-1}=2e^2\rho_0^2\delta(\omega+\omega')\int_{-\infty}^{\infty}\mathrm{d}\varepsilon(integrand2) \quad (3.28)$$

in above equation we have done this substitution $2\pi\sum_p \rightarrow \rho_0\int d\varepsilon$.

If we take the zero frequency limit (as mentioned in section 2.2.1), and if we also work in linear response regime($f_l(\varepsilon_p)=f(\varepsilon_p-\mu_l)=f(\varepsilon_p)-\mu_l\frac{\partial f}{\partial\varepsilon_p}$), we get the following simplified integrands

$$integrand1 \;=\; 8T(\varepsilon)f(\varepsilon)\left[1-f(\varepsilon)\right]$$

$$+2T(\varepsilon)(2f(\varepsilon)-1)\partial_\varepsilon f(\varepsilon)(2\mu_l+\mu_{l-1}+\mu_{l+1}) \tag{3.29}$$

and

$$\begin{aligned} integrand2 &= -4T(\varepsilon)f(\varepsilon)\left[1-f(\varepsilon)\right] \\ &\quad +2T(\varepsilon)\partial_\varepsilon f(\varepsilon)\left[1-f(\varepsilon)\right](\mu_l+\mu_{l-1}) \end{aligned} \tag{3.30}$$

we have also used equation 3.9.

Therefore the current-current correlations will be the followings:

$$\begin{aligned} S_{ll} &= 16e^2\rho_0^2\int_{-\infty}^{\infty}\mathrm{d}\varepsilon T(\varepsilon)f(\varepsilon)\left[1-f(\varepsilon)\right] \\ &\quad -4e^2\rho_0^2(2\mu_l+\mu_{l-1}+\mu_{l+1})\int_{-\infty}^{\infty}\mathrm{d}\varepsilon T(\varepsilon)\partial_\varepsilon\left[f(\varepsilon)(1-f(\varepsilon))\right] \end{aligned} \tag{3.31}$$

$$\begin{aligned} S_{ll-1} &= -8e^2\rho_0^2\int_{-\infty}^{\infty}\mathrm{d}\varepsilon T(\varepsilon)f(\varepsilon)\left[1-f(\varepsilon)\right] \\ &\quad +4e^2\rho_0^2(\mu_l+\mu_{l-1})\int_{-\infty}^{\infty}\mathrm{d}\varepsilon T(\varepsilon)\partial_\varepsilon\left(f(\varepsilon)\left[1-f(\varepsilon)\right]\right) \end{aligned} \tag{3.32}$$

As mentioned before, we are interested in zero frequency and zero temperature limit. Equations 3.31 and 3.32 are in zero frequency regime, therefore as next step we take the zero temperature limit. The only temperature dependence of these equations is in Fermi-Dirac distribution function. As $T=0$ absolute zero of temperature, the Fermi-Dirac distribution function will become a step function.

$$f(\varepsilon)=\begin{cases} 1 & : \quad \varepsilon<0 \\ 1/2 & : \quad \varepsilon=0 \\ 0 & : \quad \varepsilon>0 \end{cases}$$

When we take the zero temperature limit the function $f(\varepsilon)\,(1-f(\varepsilon))$ becomes zero everywhere except at $\varepsilon = 0$.

$$f(\varepsilon)\,(1-f(\varepsilon)) = \begin{cases} 1/4 & : \quad \varepsilon = 0 \\ 0 & : \quad \varepsilon \neq 0 \end{cases}$$

As result its derivative, will be Dirac Delta function $\delta(\varepsilon)$.

If we use the zero temperature results we will come up with

$$S_{ll} = -4e^2\rho_0^2(2\mu_l + \mu_{l-1} + \mu_{l+1})T(\varepsilon = 0) \tag{3.33}$$

$$S_{ll-1} = 4e^2\rho_0^2(\mu_l + \mu_{l-1})T(\varepsilon = 0) \tag{3.34}$$

If we consider different chemical potentials for the leads, like we did in the case of conductance, we will have

One source two drains:

$\mu_l = V/3$; $\mu_{l+1} = \mu_{l-1} = -V/3$ according to equations 3.33 and 3.34, we obtain

$S_{ll} = 0$; $S_{l+1l+1}, S_{l-1l-1} \propto -2V/3$

$S_{ll-1} = S_{ll+1} = 0$; $S_{l+1l-1} \propto -2V/3$

Two sources and one drain:

$\mu_l = \mu_{l+1} = V/3$; $\mu_{l-1} = -V/3$

consequently

$S_{ll}, S_{l+1l+1} \propto 2V/3$; $S_{l-1l-1} = 0$

$S_{ll-1} = S_{l+1l-1} = 0$; $S_{ll+1} \propto 2V/3$

We will plot $S/e^2\rho_0^2V$. Blue graphs represent intra-lead correlations and red ones represent inter-lead correlations. We utilize the data we used in previous chapter. The results are the following graphs

We see that when J crosses the critical value noise of the system goes to zero in the same way as Γ, and it follows the same tone as t increases.

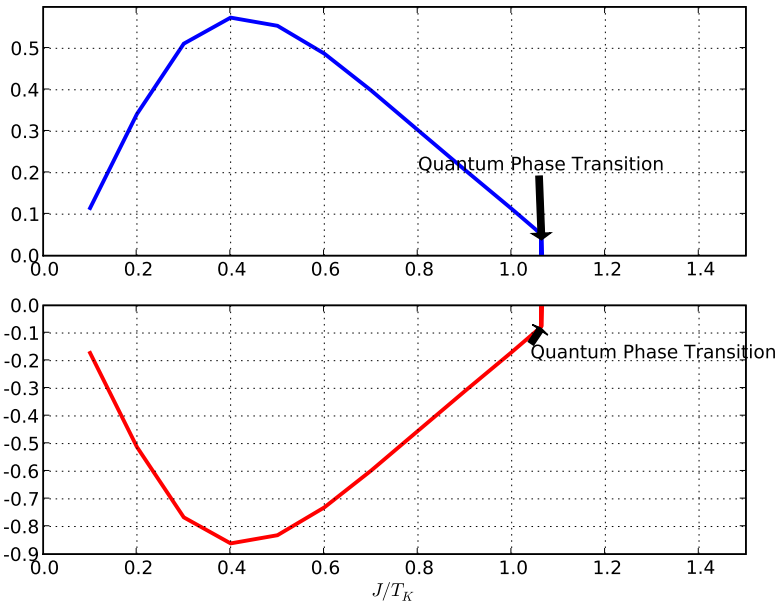

Figure 3.6: Non-zero current-current correlations in Case 1, $t = 4J$

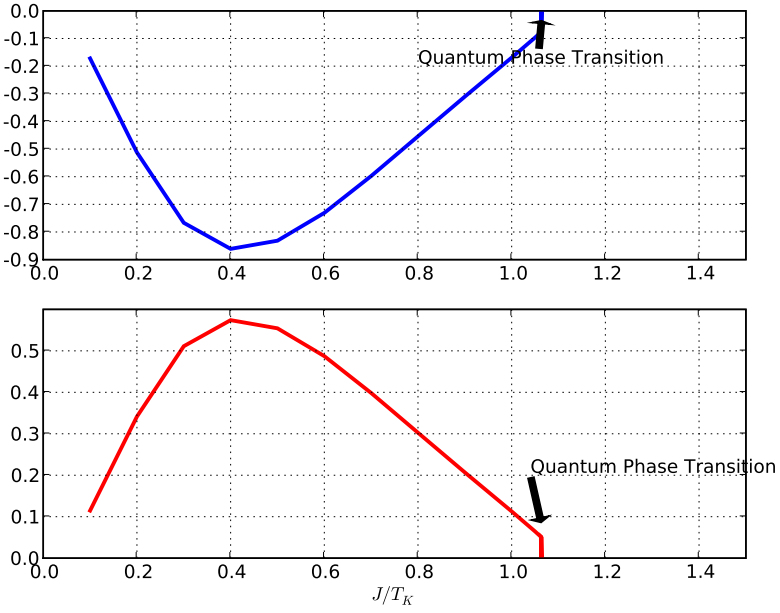

Figure 3.7: Non-zero current-current correlations in Case 2, $t = 4J$

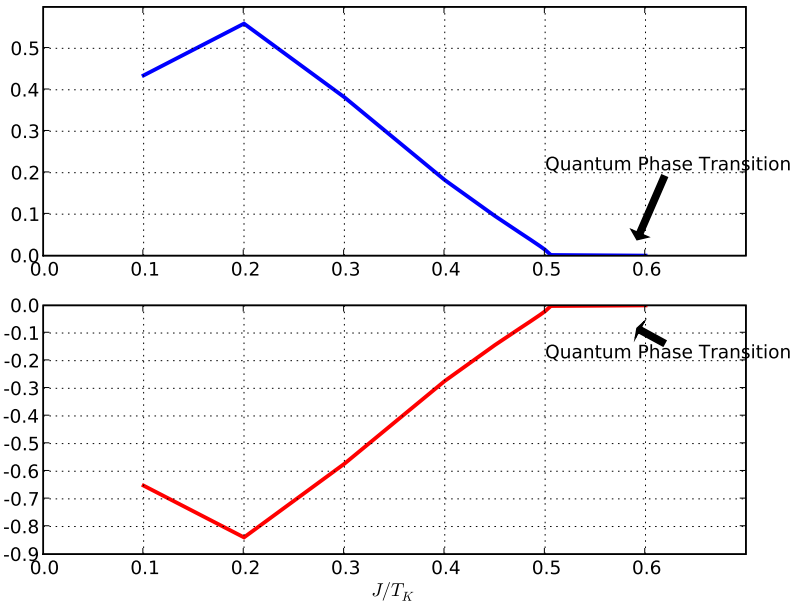

Figure 3.8: Non-zero current-current correlations in Case 1, $t = 10J$

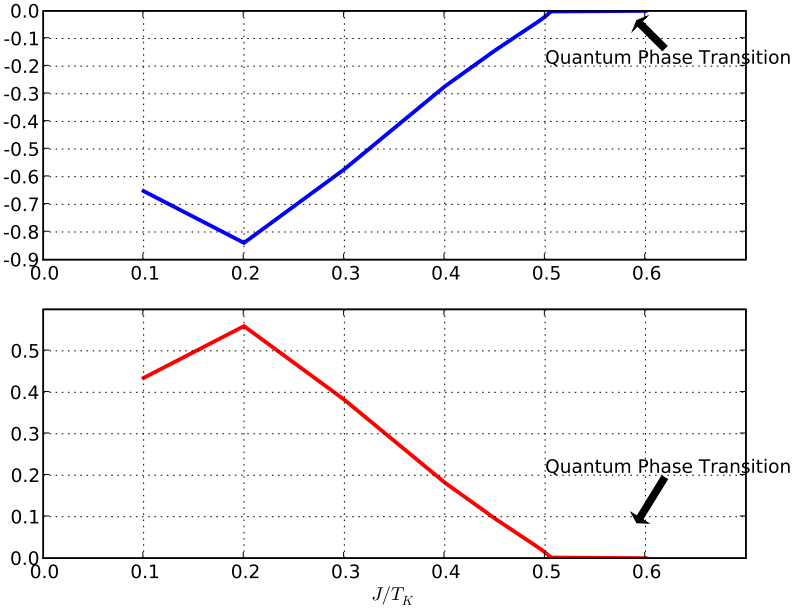

Figure 3.9: Non-zero current-current correlations in Case 2, $t = 10J$

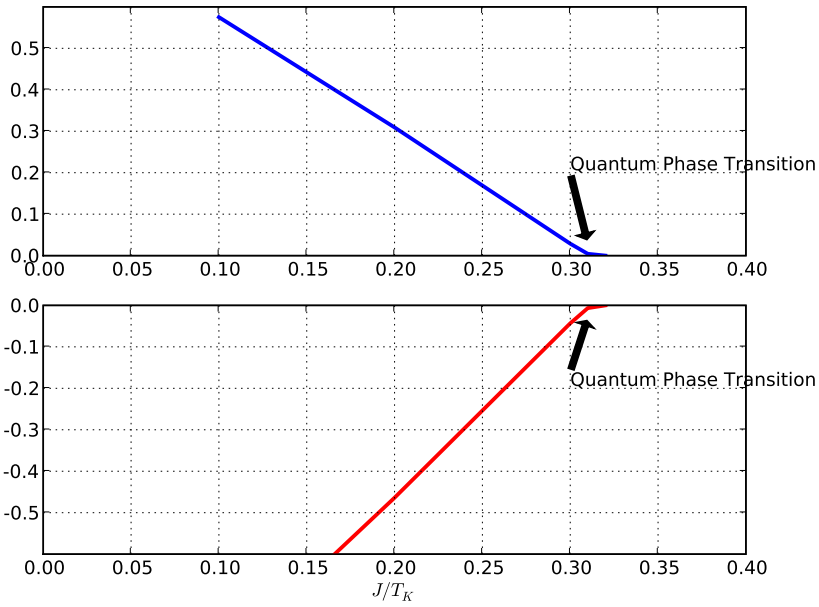

Figure 3.10: Non-zero current-current correlations in Case 1, $t = 17J$

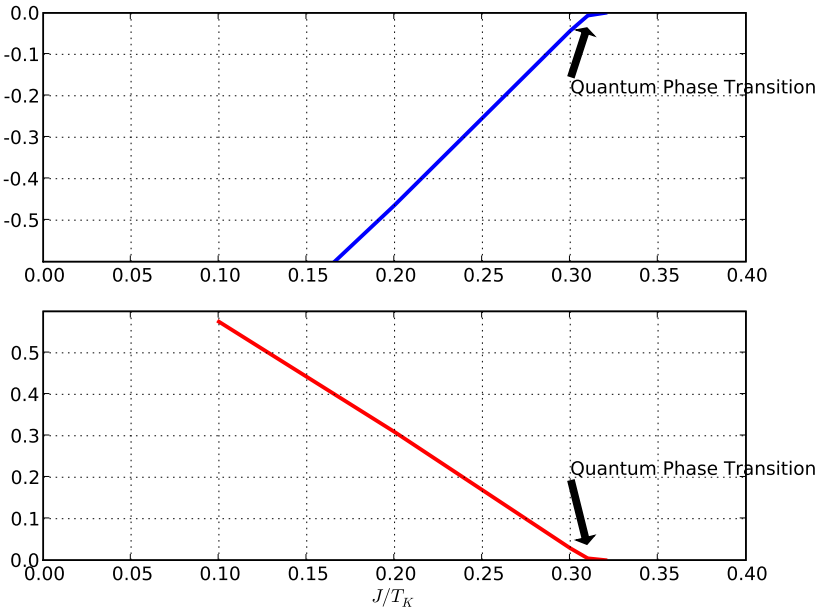

Figure 3.11: Non-zero current-current correlations in Case 2, $t = 17J$

Chapter 4

Conclusion

In this thesis, we considered the Hamiltonian of a triple quantum dot system. After integrating out the high energy degrees of freedom, we obtained the low-energy Hamiltonian (the result presented from reference [33]). After utilizing the slave-boson formalism on the low-energy Hamiltonian, we applied the Mean-Field theory to derive the physical quantities of interest in our system. The system exhibited a competition between the Kondo regime (dominant J_K Kondo coupling constant) and non-Kondo regime (dominant J). This competition yielded a quantum phase transition which the results presented in chapter two. We also investigated the influence of such a transition on the transport properties of our system (results presented in chapter three). Mean-Field results can be used to probe quantum phase transition in laboratories. As mentioned before, manufacturing of nano-structures has been progressing rapidly. As a result systems like the one we studied here can be made and used to investigate quantum phase transitions in experimental area. The value of tuning parameter J provides a reference to look for quantum phase transition.

We employed Mean-Field theory to analyze low-energy Hamiltonian of our system. As a result quantum fluctuations will be ignored. Since quantum phase transitions only happen at absolute zero of temperature, consideration of the fluctuations will change the effective low-energy Hamiltonian and consequently the transport properties. Particularly, it changes current-current correlation functions we obtained using mean-field theory. These correlations behave same as the conductance when we use mean-field theory. By considering the fluctuation we can expect to get results which reveal more details about our system. Therefore future theoretical research can be expected using stronger tools such as renormalization group to investigate the properties of quantum dot systems close to the phase boundaries.

Appendix A

Hubbard-Stratonovich Transformation

In this appendix we present the result of the low energy Hamiltonian after applying HS transformation.

After using $\vec{S}_l = \vec{S}_{ss'} f^\dagger_{ls} f_{ls'}$ and $f^\dagger, f, b^\dagger, b$ in low energy Hamiltonian 2.8we obtained

$$\begin{aligned}
H_{lowenergy} &= -t \sum_l b_{l+1} f^\dagger_{l+1s} f_{ls} b^\dagger_l + b_l f^\dagger_{ls} f_{l+1s} b^\dagger_{l+1} \\
&+ J \sum_l (\vec{S}_{ss'} f^\dagger_{l+1s} f_{l+1s'}) \cdot \vec{S}_{tt'} f^\dagger_{lt} f_{lt'}) - \frac{1}{4} (f^\dagger_{l+1s} f_{l+1s})(f^\dagger_{lt} f_{lt}) \\
&+ J' \sum_l (b_{l+1} f^\dagger_{l+1s} f_{ls'} b^\dagger_l + b_l f^\dagger_{ls} f_{l+1s'} b_{l+1}) \vec{S}_{ss'} \cdot \vec{S}_{tt'} f^\dagger_{l+2t} f_{l+2t'} \\
&- J' \sum_l \frac{1}{4} (b_{l+1} f^\dagger_{l+1s} f_{ls} b_l + b_l f^\dagger_{ls} f_{l+1s} b_{l+1}) f^\dagger_{l+2t} f_{l+2t} \\
&- \frac{J_K}{2} \sum_l (\psi^\dagger_{ls}(0) f_{ls})(f^\dagger_{ls} \psi_{ls}(0))
\end{aligned}$$

$$- \quad \frac{J'_K}{2}\sum_{i<j}(\psi^\dagger_{is}(0)f_{is}b^\dagger_i)(b_j f^\dagger_{js}\psi_{js}(0)) + (\psi^\dagger_{js}(0)f_{js}b^\dagger_j)(b_i f^\dagger_{is}\psi_{is}(0)) \quad \text{(A.1)}$$

as the next step we use the proper identities for spin operators (equation2.21)and after some simple algebra we attain equations 2.22 and 2.23. At this point we use HS transformation to get a simpler form of our low energy Hamiltonian. With use of equation 2.24 we can write the following as the last 4 terms of equation A.1

$$\begin{aligned}
&-\frac{J}{2}\Big[-|z_1|^2 - z_1(f^\dagger_{l+1s}f_{ls}) - z^*_1(f^\dagger_{lt}f_{l+1t})\Big] - \frac{J}{2}(f^\dagger_{l+1s}f_{l+1s})(1-f^\dagger_{lt}f_{lt})\\
&-\frac{J'}{2}(b_{l+1}f^\dagger_{l+1s}f_{ls}b^\dagger_l + b_l f^\dagger_{ls}f_{l+1s}b^\dagger_{l+1})(f^\dagger_{l+2t}f_{l+2t})\\
&-\frac{J'}{2}\Big[-|z_2|^2 - z_2(b_l f^\dagger_{l\uparrow}f_{l+2\uparrow} + b_{l+1}f^\dagger_{l+1\downarrow}f_{l+2\downarrow}) - z^*_2(f^\dagger_{l+2\uparrow}f_{l\uparrow}b^\dagger_l + f^\dagger_{l+2\downarrow}f_{l+1\downarrow}b^\dagger_{l+1})\Big]\\
&+\frac{J'}{2}\Big[-|z_3|^2 - z_3 b_l f^\dagger_{l\uparrow}f_{l+2\uparrow} - z^*_3 f^\dagger_{l+2\uparrow}f_{l\uparrow}b^\dagger_l\Big]\\
&+\frac{J'}{2}\Big[-|z_4|^2 - z_4 b_{l+1}f^\dagger_{l+1\downarrow}f_{l+2\downarrow} - z^*_4 f^\dagger_{l+2\downarrow}f_{l+1\downarrow}b^\dagger_{l+1}\Big]\\
&-\frac{J'}{2}\Big[-|z_5|^2 - z_5(b_l f^\dagger_{l\downarrow}f_{l+2\downarrow} + b_{l+1}f^\dagger_{l+1\uparrow}f_{l+2\uparrow}) - z^*_5(f^\dagger_{l+2\downarrow}f_{l\downarrow}b^\dagger_l + f^\dagger_{l+2\uparrow}f_{l+1\uparrow}b^\dagger_{l+1})\Big]\\
&+\frac{J'}{2}\Big[-|z_6|^2 - z_6 b_l f^\dagger_{l\downarrow}f_{l+2\downarrow} - z^*_6 f^\dagger_{l+2\downarrow}f_{l\downarrow}b^\dagger_l\Big]\\
&+\frac{J'}{2}\Big[-|z_7|^2 - z_7 b_{l+1}f^\dagger_{l+1\uparrow}f_{l+2\uparrow} - z^*_7 f^\dagger_{l+2\uparrow}f_{l+1\uparrow}b^\dagger_{l+1}\Big]\\
&+\frac{J'}{4}\Big[-|z_8|^2 - 2z_8(b_l f^\dagger_{l\uparrow}f_{l+1\uparrow}b^\dagger_{l+1} + b_{l+1}f^\dagger_{l+1\uparrow}f_{l\uparrow}b^\dagger_l + f^\dagger_{l+2\uparrow}f_{l+2\uparrow})\Big]\\
&-\frac{J'}{4}\Big[-|z_9|^2 - 2z_9(b_l f^\dagger_{l\uparrow}f_{l+1\uparrow}b^\dagger_{l+1} + b_{l+1}f^\dagger_{l+1\uparrow}f_{l\uparrow}b^\dagger_l)\Big]\\
&-\frac{J'}{4}\Big[-|z_{10}|^2 - 2z_{10}(f^\dagger_{l+2\uparrow}f_{l+2\uparrow})\Big]\\
&+\frac{J'}{4}\Big[-|z_{11}|^2 - 2z_{11}(b_l f^\dagger_{l\downarrow}f_{l+1\downarrow}b^\dagger_{l+1} + b_{l+1}f^\dagger_{l+1\downarrow}f_{l\downarrow}b_l + f^\dagger_{l+2\downarrow}f_{l+2\downarrow})\Big]\\
&-\frac{J'}{4}\Big[-|z_{12}|^2 - 2z_{12}(b_l f^\dagger_{l\downarrow}f_{l+1\downarrow}b^\dagger_{l+1} + b_{l+1}f^\dagger_{l+1\downarrow}f_{l\downarrow}b_l)\Big]\\
&-\frac{J'}{4}\Big[-|z_{13}|^2 - 2z_{13}(f^\dagger_{l+2\downarrow}f_{l+2\downarrow})\Big]\\
-\quad &\frac{J_K}{2}\sum_l\Big[-|z_{14}|^2 - z_{14}(\psi^\dagger_{ls}(0)f_{ls}) - z^*_{14}(f^\dagger_{ls}\psi_{ls}(0))\Big]
\end{aligned}$$

$$
\begin{aligned}
- \quad & \frac{J'_K}{2}\sum_{i<j}\Big[-|z_{15}|^2 - z_{15}(\psi^\dagger_{is}(0)f_{is}b^\dagger_i + \psi^\dagger_{js}(0)f_{js}b^\dagger_j) - z^*_{15}(b_j f^\dagger_{js}\psi_{js}(0) + b_i f^\dagger_{is}\psi_{is}(0))\Big] \\
+ \quad & \frac{J'_K}{2}\sum_{i=1}^{2}\Big[-|z_{16}|^2 - z_{16}\psi^\dagger_{is}(0)f_{is}b^\dagger_i - z^*_{16}b_i f^\dagger_{is}\psi_{is}(0)\Big] \\
+ \quad & \frac{J'_K}{2}\sum_{j=2}^{3}\Big[-|z_{17}|^2 - z_{17}\psi^\dagger_{js}(0)f_{js}b^\dagger_j - z^*_{17}b_i f^\dagger_{js}\psi_{js}(0)\Big] \qquad \text{(A.2)}
\end{aligned}
$$

the last three terms of equation A.2 represent the fifth term of equation A.1 where we have used the identity $AB + B^\dagger A^\dagger = (A + B^\dagger)(A^\dagger + B) - AA^\dagger - B^\dagger B$.(A and B can be $\psi^\dagger_{ls}(0)f_{ls}b^\dagger_l$ and $b_i f^\dagger_{is}\psi_{is}(0)$).

Appendix B

Symmetries and Their Consequences

As mentioned in chapter one, because our system has a fully triangular symmetry our mean fields can be chosen real.

B.1 Case of $\eta =< f^{\dagger}_{l+1\sigma} f_{l\sigma} >$:

We consider a unitary transformation operator u. We define u as $u^{\dagger} c_1 u = c_2$ where c_i are dot annihilation operators. Under this operation the Hamiltonian of our system is invariant because of the triangular symmetry. $u^{\dagger} H u = H$ where $H = H_{lowenergy}$. We can see this invariance to switching indices of dot operators in equation B.1 (first three terms)

$$H_{lowenergy} = -t \sum_{l} c^{\dagger}_{l+1s} c_{ls} + c^{\dagger}_{ls} c_{l+1s}$$

$$
\begin{aligned}
&+ \quad J\sum_{l}\vec{S}_{l+1}\cdot\vec{S}_{l}-\frac{1}{4}n_{l+1}n_{l}\\
&+ \quad J'\sum_{l}(c^{\dagger}_{l+1s}c_{ls'}+c^{\dagger}_{ls}c_{l+1s'})\vec{S}_{ss'}\cdot\vec{S}_{l+2}-\frac{1}{4}(c^{\dagger}_{l+1s}c_{ls}+c^{\dagger}_{ls}c_{l+1s})n_{l+2}\\
&- \quad \frac{J_K}{2}\sum_{l}(\psi^{\dagger}_{ls}(0)f_{ls})(f^{\dagger}_{ls}\psi_{ls}(0))\\
&- \quad \frac{J'_K}{2}\sum_{i<j}(\psi^{\dagger}_{is}(0)f_{is}b^{\dagger}_{i})(b_jf^{\dagger}_{js}\psi_{js}(0))+(\psi^{\dagger}_{js}(0)f_{js}b^{\dagger}_{j})(b_if^{\dagger}_{is}\psi_{is}(0)) \quad \text{(B.1)}
\end{aligned}
$$

After applying mean field theory and entering the auxiliary fields, our Hamiltonian will include terms of the form $\eta f^{\dagger}_1 f_2+\eta^* f^{\dagger}_2 f_1$ where η is the same mean field introduced in chapter one ($\eta =< f^{\dagger}_{l+1\sigma}f_{l\sigma} >$). These terms and the invariability of Hamiltonian to the unitary transformation u(we introduced above) force η to be real as the following

$u^{\dagger}Hu = H \rightarrow \eta f^{\dagger}_1 f_2+\eta^* f^{\dagger}_2 f_1 = \eta f^{\dagger}_2 f_1+\eta^* f^{\dagger}_1 f_2 \Rightarrow \eta = \eta^*$.

B.2 Case of $\chi =< \psi^{\dagger}_{l\sigma}f_{l\sigma} >$:

In this case we first assume that χ is not real. Consequently we can write $\chi = |\chi|\, e^{i\theta} \Rightarrow |\chi| =< e^{-i\theta}\psi^{\dagger}_{l\sigma}f_{l\sigma} >$. So we consider a phase for our second quantized operator ψ. This phase is the same for all lead operators because we have assumed that they are completely similar. We define $\psi'_{l\sigma} = e^{i\theta}\psi_{l\sigma}$. If we consider fourth and fifth terms of the low energy Hamiltonian and Hamiltonian of the leads

$$
\begin{aligned}
&- \quad \frac{J_K}{2}\sum_{l}(\psi^{\dagger}_{ls}(0)f_{ls})(f^{\dagger}_{ls}\psi_{ls}(0))\\
&- \quad \frac{J'_K}{2}\sum_{i<j}(\psi^{\dagger}_{is}(0)f_{is}b^{\dagger}_{i})(b_jf^{\dagger}_{js}\psi_{js}(0))+(\psi^{\dagger}_{js}(0)f_{js}b^{\dagger}_{j})(b_if^{\dagger}_{is}\psi_{is}(0))\\
&- \quad iv_F\sum_{l}\int_{-L}^{L}dx\psi^{\dagger}_{l}\partial_x\psi_{l} \quad \text{(B.2)}
\end{aligned}
$$

we can see they are only terms which depend on ψ. Their structure allows us to substitute ψ' for ψ without changing the physical characteristic of our Hamitonian.

As a result we can always have a real $\chi =< \psi^{\dagger}_{l\sigma} f_{l\sigma} >$ just by choosing a proper phase for our second quantized lead operator ψ.

Appendix C

Relation between Spectral Density and Thermal Occupation

In this appendix we show how spectral density is related to the thermal occupation. In other words we have to show how one can get the following equation

$$< f^{\dagger}_{l+1\sigma} f_{l\sigma} >= \frac{1}{2\pi} \int_{-\infty}^{\infty} d\omega f(\omega) B(\omega) \tag{C.1}$$

where

$$\begin{aligned} B(\omega) &= -2Im(\tilde{G}(\omega)) \\ \tilde{G}(\omega) &= \int_{-\infty}^{\infty} dt e^{i\omega t} \tilde{G}(t) \\ \tilde{G}(t) &= -i\theta(t) < \{f_{l\sigma}(t), f^{\dagger}_{l+1\sigma}\} > \end{aligned} \tag{C.2}$$

here

$$f_{l\sigma}(t) = e^{iHt} f_{l\sigma} e^{-iHt} \tag{C.3}$$

and

$$< \{f_{l\sigma}(t), f^{\dagger}_{l+1\sigma}\} >= \frac{1}{Z} Tr\left[e^{-\beta H}\{f_{l\sigma}(t), f^{\dagger}_{l+1\sigma}\}\right] \tag{C.4}$$

we perform the trace using eigenstates of the full Hamiltonian. These eigenstates exist but in general we do not know what they are. After inserting equations C.3 and C.4 $\tilde{G}(t)$ expression and using Identity $I = \sum_n |n><n|$ we obtain

$$\begin{aligned}\tilde{G}(t) = -i\theta(t)\frac{1}{Z}\sum_{mn} \quad & e^{-\beta E_m} e^{i(E_m - E_n)t} < m\,|f_{l\sigma}|\,n >< n\left|f^{\dagger}_{l+1\sigma}\right| m > \\ & + e^{-\beta E_m} e^{i(E_n - E_m)t} < m\left|f^{\dagger}_{l+1\sigma}\right| n >< n\,|f_{l\sigma}|\,m > \end{aligned} \tag{C.5}$$

If we switch the role of m and n in the second term of equation C.5, we get

$$\tilde{G}(t) = -i\theta(t)\frac{1}{Z}\sum_{mn}(e^{-\beta E_m} + e^{-\beta E_n}) e^{i(E_m - E_n)t} < m\,|f_{l\sigma}|\,n >< n\left|f^{\dagger}_{l+1\sigma}\right| m > \tag{C.6}$$

Now we perform Fourier transform $\tilde{G}(\omega) = \int_{-\infty}^{\infty} dt e^{i\omega t}\tilde{G}(t)$ to get

$$\tilde{G}(\omega) = \frac{-i}{Z}\sum_{mn}(e^{-\beta E_m} + e^{-\beta E_n}) < m\,|f_{l\sigma}|\,n >< n\left|f^{\dagger}_{l+1\sigma}\right| m > \int_{-\infty}^{\infty} \theta(t) e^{i(E_m - E_n + \omega)t} dt \tag{C.7}$$

by performing the integration we get

$$\begin{aligned}\int_{-\infty}^{\infty} \theta(t) e^{i(E_m - E_n + \omega + i\delta)t} dt &= \frac{-i}{E_m - E_n + \omega + i\delta} e^{i(E_m - E_n + \omega + i\delta)t}|_0^{infty} \\ &= iP(\frac{1}{E_m - E_n + \omega}) + \pi\delta(E_m - E_n + \omega)\end{aligned} \tag{C.8}$$

where we added $i\delta$ to avoid divergence and then we took the limit $\delta \to 0$. We also used $\lim_{\delta\to 0}\frac{1}{x+i\delta} = P(\frac{1}{x}) - i\pi\delta(x)$.

Consequently we will have

$$\begin{aligned}\tilde{G}(\omega) = \frac{1}{Z}\sum_{mn} \quad & (e^{-\beta E_m} + e^{-\beta E_n}) < m\,|f_{l\sigma}|\,n >< n\left|f^{\dagger}_{l+1\sigma}\right| m > \\ & \times\left[P(\frac{1}{E_m - E_n + \omega}) - i\pi\delta(E_m - E_n + \omega)\right]\end{aligned} \tag{C.9}$$

using $B(\omega) = -2Im(\tilde{G}(\omega))$ we get

$$B(\omega) = \frac{2\pi}{Z}\sum_{mn}(e^{-\beta E_m} + e^{-\beta E_n}) < m\,|f_{l\sigma}|\,n >< n\left|f^{\dagger}_{l+1\sigma}\right|m > \delta(E_m - E_n + \omega) \quad \text{(C.10)}$$

The final step to show the relation C.1 is to perform the integration $\frac{1}{2\pi}\int_{-\infty}^{\infty} d\omega f(\omega)B(\omega)$

$$\begin{aligned}
\frac{1}{2\pi}\int_{-\infty}^{\infty} d\omega f(\omega)B(\omega) &= \frac{1}{Z}\sum_{mn} < m\,|f_{l\sigma}|\,n >< n\left|f^{\dagger}_{l+1\sigma}\right|m > \\
&\quad \times \int_{-\infty}^{\infty} \delta(E_m - E_n + \omega)(e^{-\beta E_m} + e^{-\beta E_n})f(\omega)d\omega \\
&= \frac{1}{Z}\sum_{mn} < m\,|f_{l\sigma}|\,n >< n\left|f^{\dagger}_{l+1\sigma}\right|m > \frac{e^{-\beta E_m} + e^{-\beta E_n}}{e^{-\beta(E_m - E_n)}} \\
&= \frac{1}{Z}\sum_{mn} < m\,|f_{l\sigma}|\,n >< n\left|f^{\dagger}_{l+1\sigma}\right|m > e^{-\beta E_n} \\
&= \frac{1}{Z}\sum_{n} < n\left|e^{-\beta H} f^{\dagger}_{l+1\sigma} f_{l\sigma}\right|n > \\
\frac{1}{2\pi}\int_{-\infty}^{\infty} d\omega f(\omega)B(\omega) &= < f^{\dagger}_{l+1\sigma} f_{l\sigma} > \qquad \text{(C.11)}
\end{aligned}$$

The proof is complete now.

Appendix D

Integrals containing Fermi-Dirac Distribution Function

In this appendix we show how one can get one dimensional Dirac Hamiltonian from the regular second quantized Hamiltonian we used. (2.2)

$$H_{leads} = \sum_{l} \sum_{p} \varepsilon_p c^{\dagger}_{lps} c_{lps} \tag{D.1}$$

As mentioned, we have considered the conduction electrons in the leads as plane waves. As a consequence, their energy will be the free particle energy $\varepsilon_p = \frac{p^2}{2m}$. Since we are interested in $T = 0$ regime, these electrons are very close to the Fermi surface and so is their energy to Fermi energy. According to this we can approximate ε_p as

$$\begin{aligned} \varepsilon_p &= \frac{p^2}{2m} = \frac{(p - p_F + p_F)^2}{2m} \\ &= \frac{(p - p_F)^2 + p_F^2 + 2pp_F}{2m} \approx \frac{p_F^2}{2m} + \frac{pp_F}{m} \end{aligned}$$

$$\varepsilon_p \approx \frac{p_F^2}{2m} + \frac{pp_F}{m} \tag{D.2}$$

where we eliminated $(p-p_F)^2$ because it is very small in $T=0$ regime. $p_F = \sqrt{2mE_F}$ (Fermi momentum) where E_F is Fermi energy. We can also define Fermi velocity as $v_F = \frac{p_F}{m}$. First term of final equation of D.2 is also Fermi energy. So if we consider our energy reference point at Fermi surface we will obtain the following relation as our electron energy in $T=0$ regime

$$\varepsilon_p \approx v_F p \tag{D.3}$$

We can also write equation D.1 in the form of

$$H_l eads = \sum_l \sum_{pp'} \varepsilon_p c^\dagger_{lp's} c_{lps} \delta(p-p') \tag{D.4}$$

if we insert the Fourier transform of Delta function $\delta(p-p') = \frac{1}{V}\int_{-\infty}^{\infty} e^{i(p-p')x}dx$, after some rearrangements we obtain

$$\begin{aligned} H_{leads} &= \sum_l \int_{-\infty}^{\infty} dx v_F \frac{1}{\sqrt{V}} \sum_{p'} c^\dagger_{lp's} e^{-ip'x} \frac{1}{\sqrt{V}} \sum_p p c_{lps} e^{ipx} \\ &= \sum_l \int_{-\infty}^{\infty} dx v_F \frac{1}{\sqrt{V}} \sum_{p'} c^\dagger_{lp's} e^{-ip'x} (-i\partial_x) \frac{1}{\sqrt{V}} \sum_p c_{lps} e^{ipx} \\ H_{leads} &= -iv_F \sum_l \int_{-\infty}^{\infty} dx \psi^\dagger_{ls}(x) \partial_x \psi_{ls}(x) \end{aligned} \tag{D.5}$$

which is the Dirac Hamiltonian.

Appendix E

Numerical Calculations: Methods and Results

In this appendix we present the code we have used to find the roots of our equations 2.50 self-consistently. The code has been written in Python.

A common method to solve equations self-consistently is Broyden's formalism. The code of this method is part of the library of Python. We practically call this formalism in our code. Broyden's formalism needs initial seeds to start solving the equations. In fact these initial seeds are user's guess for the roots of equations. The method is very sensitive to the choice of initial seeds.

We are interested in finding the roots for different values of J. As a result of this we will be able to probe the quantum phase transition. In our code as we can see, we sweep different initial seeds for a particular value of J in an interval which is reasonable enough to find the solutions in. The code sweeps different initial conditions and writes the solutions into a file. Because we are dealing with mean-field variables,

the solutions in the interval [0,1] will only be chosen.(we can see in the code)

As the first step, different values of J are considered. The only acceptable J values are the ones which give the answers in the interval of interest. The next step is to choose the proper roots resulting from different initial conditions. This is the most important step. This has to yield quantum phase transition and the same results as we presented in chapter 2.

The code:

```
from numpy import *
from scipy import optimize
def g(x):
return numpy.array(x)
t=open('Dataphase2', 'w')
J=1.8
l10=1.36*J
l11=-0.042*J
l12=1.17*J
l20=-2.72*J
l21=0.083*J
l22=-2.08*J
def F(g):
    f1 = g[0]-0.5+0.21*arctan((l10+l11*g[0]+l12*g[1])/g[2])
+0.11*arctan((l20+l21*g[0]+l22*g[1])/g[2])
    f2 = g[1]-0.11*arctan((l10+l11*g[0]+l12*g[1])/g[2])
+0.11*arctan((l20+l21*g[0]+l22*g[1])/g[2])
    f3 =((l10+l11*g[0]+l12*g[1])**2+g[2]**2)
*sqrt(g[2]**2+(l20+l21*g[0]+l22*g[1])**2)-1
    return (f1, f2, f3)
```

```
for k in range(26):
    for l in range(26):
        for m in range(26):
            k1=-2.5+k*0.2
            l1=-2.5+l*0.2
            m1=-2.5+m*0.2
            w=optimize.broyden2(F, (k1,l1,m1), iter=45)
            r=w.copy()
            if r[0,0]>0 and r[0,0]<1.1:
                if r[0,1]>0 and r[0,1]<1.1:
                    if r[0,2]>-0.0000001 and r[0,2]<1.0000001:
                        o="".join(map(str,r))
                        p2=str(k1)
                        p3=str(l1)
                        p4=str(m1)
                        t.write(p2)
                        t.write(")
                        t.write(p3)
                        t.write(")
                        t.write(p4)
                        t.write(")
                        t.write(o)
                        t.write(")
                        t.write(")
t.close()
```

in this code g[i] (i=0,1,2) represents our mean-field variables of interest.

We expect when J increases the Kondo mean-field variable decreases and also η

increases. This is the key to choose roots as an answer among many, for a particular value of J. I tried to do this manually. It is very time consuming and slow. The best results I could get so far, will be presented below. These ones have been chosen just by looking at the Kondo mean-field variable. If one considers the other mean-field variable, η, these results can be adjusted and will yield to the proper answers.

Results for Kondo mean-field variable:

J	Γ
0.999405020299	7.245e-5
0.99940502	1.741e-4
0.99940501	3.84e-4
0.999405	0.00087733
0.9994	0.00171872
0.9993	0.00533204
0.9992	0.00825543
0.9991	0.08455616
0.999	0.128455
0.996	0.385612
0.993	0.447563
0.992	0.516736
0.991	0.588249
0.99	0.611904
0.98	0.631859
0.97	0.664367
0.96	0.744958
0.95	0.765239
0.94	0.780348
0.93	0.782575
0.92	0.83249
0.91	0.838999
0.90	0.852618

References

[1] L. Kouwenhoven and L. Glazman. Revival of kondo effect. *Physics World*, pages 33–38, January 2001.

[2] Y. Murayama. *Mesoscopic Systems, Fundamentals and Applications*. Wiley-VCH, 2001.

[3] M. A. Kastner. Artificial atoms. *Physics Today*, 46(1):24–31, 1993.

[4] P. McEuen. Single-wall carbon nanotubes. *Physics World*, pages 31–36, June 2000.

[5] M. Sigrist, T. Ihn, M. Reinwald, and W. Wegscheider. Coherent probing of excited quantum dot states in an interferometer. *Phys. Rev. Lett.*, 98(036805), 2007.

[6] R. Schuster, E. Buks, M. Heiblum, D. Mahalu, V. Umansky, and H. Shtrikman. Phase measurement in a quantum dot via a double-slit interference experiment. *Nature*, 385:417–420, 1997.

[7] J. Konig and Y. Gefen. Aharanov-bohm interferometery with interacting quantum dots. *Phys. Rev. B*, 65(045316), 2002.

[8] A. N. Korotkov. Output spectrum of a detector measuring quantum oscillations. *Phys. Rev. B*, 63(085312), 2001.

[9] A. N. Korotkov. Selective quatum evolution of a qubit state due to continuous measurement. *Phys. Rev. B*, 63(115403), 2001.

[10] W. D. Oliver, F. Yamaguchi, and Y. Yamamoto. Electron entanglement via a quantum dot. *Phys. Rev. Lett.*, 88(3), 2002.

[11] F. Kuemmeth, S. Ilani, D. C. Ralph, and P. L. McEuen. Coupling of spin and orbital motion of electrons in carbon nanotubes. *Nature*, 452(06822), 2008.

[12] Q. Ho-Kim, C. S. Lam, and Kumar N. *Invitation to Contemporary Physics*. World Scientific, 2004.

[13] M. Braun, J. Konig, and J. Martinek. Theory of transport through quantum-dot in the weak coupling regime. *Phys. Rev. B*, 70(195345), 2004.

[14] I. Affleck and E. Sela. Nonqulibrium transport through double quantum dots:exact results near quantum critical point. *Phys. Rev. Lett.*, 102(047201), 2009.

[15] A. Georges and Y. Meir. Electronic correlations in transport through coupled quantum dots. *Phys. Rev. Lett.*, 82(17), 1999.

[16] L. G. G. V. Dias da Silve, N. Sandler, P. Simon, K. Ingersent, and Ulloa S. E. Finite-temperature conductance signatures of quantum criticality in double quantum dots. *Phys. Rev. B*, 78(153304), 1999.

[17] R. Zitko and J. Bonca. Multiple-impurity anderson model for quantum dots coupled in parallel. *Phys. Rev. B*, 74(045312), 2006.

[18] P. Schlottmann and Zvyagin A. A. t-j ring with an anderson impurity : A model for a quantum dot. *Phys. Rev. B*, 67(115113), 2003.

[19] A. C. Hewson. *The Kondo problem to Heavy Fermions*. Cambridge University Press, 1993.

[20] M. Vojta, R. Bulla, and W. Hofstetter. Quantum phase transitions in models of coupled magnetic impurities. *Phys. Rev. B*, 64(140405), 2002.

[21] B. A. Jones, B. G. Kotliar, and A. J. Milis. Mean-field analysis of two antiferromagnetically coupled anderson impurities. *Phys. Rev. B*, 39(5 (Rapid Communications)), 1989.

[22] C. H. Chung, M. T. Glossop, L. Fritz, M. Kircan, and M. Vojta. Quantum phase transitions in a resonant level model with dissipation:renormalizatin-group studies. *Phys. Rev. B*, 76(235103), 2007.

[23] N. Roch, S. Florens, V. Bouchiat, W. Wernsdorfer, and F. Balestro. Quantum phase transition in a single-molecule quantum dot. *Nature*, 453:633–638, 2008.

[24] M. Eto and V. Nazarov. Mean field theory of the kondo effect in quantum dots with an even number of electrons. *cond-matt/0101152v*, 2001.

[25] N. J. Craig, J. M. Taylor, C. M. Marcus, M. P. Hanson, and Gossard A. C. Tunable nonlocal spin control in a coupled-quantum dot system. *Science*, 304:565–567, 2004.

[26] S. M. Cronenwett, T. H. Oosterkamp, and L. P. Kouwenhoven. A tunable kondo effect in quantum dots. *Science*, 304:540–543, 1998.

[27] S. Sasaki, N. De Franceschi, W. G. van der Viel, M. Eto, Tarucha S., and L.P. Kouwenhoven. Kondo effect in an integer-spin quantum dot. *Nature*, 405:764–767, 2000.

[28] K. Kikoin and Y. Avishai. Kondo physics in artificial molecules. *cond-matt/0612028 v1*, 2006.

[29] L. G. G. V. Dias da Silve, N. Sandler, P. Simon, K. Ingersent, and Ulloa S. E. Tunable pseudogap kondo effect and quantum phase transitions in aharonov-bohm interferometers. *Phys. Rev. Lett.*, 102(166806), 2009.

[30] R. K. Pathria. *Statistical Mechanics, Second Edition*. Butterworth-Heinemann, 1996.

[31] S. L. Sondhi, S. M. Girvin, J. P. Carini, and Sahar D. Continuous quantum phase transitions. *Review of Modern Physics*, 69(1), 1997.

[32] S. Sachdev. *Quantum Phase Transitions*. Cambridge University Press, 2001.

[33] E. H. Kim. Effective low energy hamiltonian. *Unpublished*, 2009.

[34] K. Huang. *Statistical Mechanics*. John Wiley and Sons, 1987.

[35] M. Buttiker. Scattering theory of current and intensity noise correlations in conductors and wave guides. *Phys. Rev. B*, 46(19), 1992.

[36] M. Buttiker. Role of scattering amplitudes in frequency-dependent current fluctuations in small conductors. *Phys. Rev. B*, 45(7), 1992.

[37] I. S. Gradshteyn and I. M. Ryzhnik. *Tables of Integrals, Series and Products*. Academic Press, Inc, 1992.

[38] A. L. Fetter and J. D. Walecka. *Quantum Theory of Many-Particle Systems*. McGraw-Hill Book Company, 1971.

[39] R. W. Byron Jr, F. W. Fuller. *Mathematics of Classical and Quantum Physics Volume Two*. Addison-Wesley Publishing Company, 1970.

VITA AUCTORIS

Behnam Javanparast was born in 1983 in Rasht, Gilan, Iran. He graduated from Mirza Kouchak Khan(National Organization of Exceptional Talents Center in Rasht) in 2001. He obtained his B.Sc. in Physics in 2006 from Sharif University of Technology and his M.Sc. in 2009 from University of Windsor.